

# **MnO<sub>4</sub> – Fe(III) dosing to rapid sand filters for removing arsenic from drinking water to <1 µg/l**

## ***A case study in Katwijk (Dunea)***

Brent Pieterse

For the degree of:  
***Master of Science in Civil Engineering***

Date of submission:  
14-12, 2017

Date of defense:  
21-12, 2017

Examination Committee:

Prof.dr.ir L.C. Rietveld	Delft University of Technology Section Sanitary Engineering
Dr.ir D. van Halem	Delft University of Technology Section Sanitary Engineering
Dr.ir G.H.W. Schoups	Delft University of Technology Section Water Resources
A. Ahmad, MSc	KWR Water cycle research institute Water Systems and Technology Group
Ing. W.A. Oorthuizen	Dunewater company Dunea N.V. Assetmanagement Technology

Section Sanitary Engineering, Department of Water Management  
Faculty of Civil Engineering and Geosciences  
Delft University of Technology  
Delft, the Netherlands



## Abstract

Drinking water company Dunea N.V. produces drinking water by artificially infiltrating water into the dunes. During this dune passage arsenic is mobilized causing arsenic levels up to 4 µg/l in the influent of DWTP Katwijk. In this thesis the effectiveness of the  $\text{MnO}_4 - \text{Fe(III)}$  dosing was evaluated on RSF influent of Dunea's treatment plant Katwijk. The goal of the experiments was to reduce the residual arsenic concentration to <1µg/l while minimizing negative effects on further treatment steps. Experiments were performed in a pilot filter filled with filter material originating from the RSFs in Katwijk to ensure conditions were similar to RSFs in Katwijk. The performance of  $\text{MnO}_4 - \text{Fe(III)}$  dosing was evaluated at different filtration velocities (4, 6, 10 m/h) and at different top layer materials (anthracite (1.6-2.5mm) and pumice (2.5-3.5mm)).

In this research multiple dosages were evaluated and residual As <1µg/l was consistently achieved by dosing 0.5 mg  $\text{NaMnO}_4$  /l and 1.0 mg Fe(III) /l. It was found that the effectiveness of the  $\text{MnO}_4 - \text{Fe(III)}$  dosing was not influenced by the filtration velocity applied in the RSFs. For all the filtration velocities checked the removal efficiency ranged from 60-70%, resulting in As levels <1µg/l. The pumice used appeared to show slightly higher removal rates than the anthracite that was used. However, for full scale application purposes in Katwijk the used anthracite was better suited. The pumice filter clogged faster leading to a pressure loss of 95 cmWc after 6 days while the anthracite filter reached a pressure loss of 73 cmWc. Due to the coarse top layer less particles were removed in the top layer and caused the sand underneath to be loaded more and to clog more quickly.

The AOCF process did not negatively influence the filter performance. Mn-, Fe- removal and nitrification all still performed to standards and the turbidity of the RSF effluent decreased from 0.3 FTU to 0.03 FTU. Based on preliminary experiments the sedimentation properties of the backwash water changed and the sedimentation velocity increased.

The  $\text{MnO}_4$ -Fe(III) dosage can effectively reduce the residual arsenic concentration to <1µg/l and is ready to be applied at Katwijk. However, the negative effects on the runtime of the RSFs can't be overlooked. The runtime of the current filters is expected to decrease by about 50% causing a higher stress on the backwash water treatment.



## **Preface**

This thesis is the result of a 10 month research I performed at DWTP Katwijk for my graduation for my MSc. I am really thankful for the opportunity to work on this project at Dunea and hope that the research contributed to the overall project on removing arsenic from drinking water.

I want to thank everyone that contributed to any part of my work. I want to particularly thank my my daily supervisors Wim Oorthuizen and Arslan Ahmad for the supervision while doing my pilot experiments. Discussions about obtained results really helped me draw conclusions.

Furthermore I really want to thank my supervisors from the TU Delft. Doris van Halem and Luuk Rietveld both helped me greatly when I was a bit lost with the direction of my MSc thesis. I really want to thank them for the support they gave me and setting me on the right path again.

## List of figures

- Figure 1: Drinking water scheme from source to drinking water
- Figure 2: pH – Eh diagram of arsenic compounds
- Figure 3: Various filtration mechanisms
- Figure 4: Lindquist diagrams in single media filtration
- Figure 5: Lindquist diagrams in multi-layer filtration
- Figure 6: AOCF jar test results
- Figure 7: Pilot installation used in experiments
- Figure 8: Equipment used for turbidity and pH measurements
- Figure 9: Tracer experiment performed
- Figure 10: As speciation over the height of a RSF in Katwijk
- Figure 11: As speciation over the height of the anthracite pilot filter
- Figure 12: Fe and Mn removal in the RSF in Katwijk
- Figure 13: Nitrification, denitrification and phosphate removal in the RSF in Katwijk
- Figure 14: Dissolved As in the pumice filter
- Figure 15: Dissolved As in the anthracite filter
- Figure 16: As(III) behavior over filter height while applying AOCF
- Figure 17: Normalized Lindquist diagram for the anthracite filter
- Figure 18: Normalized Lindquist diagram for the pumice filter
- Figure 19: Comparison of pressure loss between the pumice and anthracite filter at a filtration velocity of 4 m/h
- Figure 20: Breakthrough of the anthracite filter with and without AOCF
- Figure 21: Breakthrough of the pumice filter at varying filtration velocities
- Figure 22: Volume treated before breakthrough is reached
- Figure 23: Backwash water experiment results
- Figure 24: Backwash water turbidity measurements
- Figure 25: Backwash water settling velocity measurements
- Figure 26: Secondary backwash experiment at  $T = 8$  mins
- Figure 27: Secondary backwash experiment at  $T = 26$  mins
- Figure 28: Pressure loss of the pilot compared to the RSFs in Katwijk without AOCF
- Figure 29: Lindquist diagram of the anthracite filter at a filtration velocity of 4 m/h
- Figure 30: Lindquist diagram of the pumice filter at a filtration velocity of 4 m/h
- Figure 31: Normalized Lindquist diagram of the anthracite filter at a filtration velocity of 6 m/h
- Figure 32: Normalized Lindquist diagram of the anthracite filter at a filtration velocity of 10 m/h
- Figure 33: Normalized Lindquist diagram for the pumice filter at 6 m/h
- Figure 34: Normalized Lindquist diagram of the Pumice filter at a filtration velocity of 10 m/h
- Figure 35: Backwash experiment turbidity at 750 ml (no AOCF)
- Figure 36: Backwash experiment turbidity at 750 ml (AOCF applied)

## List of tables

Table 1: As during drinking water production from source to plant effluent at WTP Katwijk (Dunea, 2016).

Table 2: Backwash regime used in pilot experiments.

Table 3: Experiments performed and important parameters

Table 4: Dosing optimization experiment

Table 5: Dosing optimization results

Table 6: Average As removal efficiency at various filtration velocities in the pumice filter

Table 7: Average As removal efficiency at various filtration velocities in the anthracite filter

Table 8: Estimated contact time in the layers of the pilot filter

Table 9: All pressure loss results

Table 10: Ammonium, nitrate, nitrite and Mn removal in the pilot and RSFs in Katwijk

## List of abbreviations

AOCF	:	Advanced Oxidation Coagulation Filtration
As	:	Arsenic
DWTP	:	Drinking Water Treatment Plant
Dunea	:	Dunea Duin & Water
HWL	:	Het Waterlaboratorium
ICP-MS	:	Inductively coupled plasma mass spectrometry
PAC	:	Powdered Activated Carbon
RSF	:	Rapid Sand Filtration
SSF	:	Slow Sand Filtration
USEPA	:	Environmental Protection Agency of United States
VEWIN	:	Vereniging van Waterbedrijven In Nederland
WHO	:	World Health Organization

## Table of contents

1. Introduction.....	10
1.1 Arsenic in drinking water in the Netherlands.....	10
1.2 Arsenic in drinking water at WTP Katwijk and its source .....	10
1.2.1 Treatment of dune effluent at DWTP Katwijk .....	10
1.2.2 Dune infiltration.....	11
1.2.3 Powdered Activated Carbon dosage .....	11
1.2.4 Cascade Aeration.....	11
1.2.5 Pellet softening.....	12
1.2.6 Rapid Sand Filtration.....	12
1.2.7 Backwash water treatment.....	12
1.2.8 Slow sand filtration .....	12
1.3. Scope of this thesis .....	13
1.3.1 Objectives.....	13
1.3.2 Research questions .....	13
1.3.3 Thesis content .....	14
2. Literature Review .....	15
2.1 Arsenic speciation.....	15
2.2 Previous research: iron dosing in Katwijk .....	16
2.3 Advanced Oxidation Coagulation Filtration (AOCF) .....	16
2.3.1 Different oxidants.....	16
2.3.2 Different coagulants .....	17
2.4 Rapid Sand Filtration (RSF).....	17
2.5 Previous AOCF research at Dunea on As removal .....	20
2.5.1 AOCF Jar Tests.....	20
2.5.2 Construction of the AOCF pilot filter.....	21
3. Materials and methods .....	22
3.1 Pilot setup .....	22
3.1.1 Pilot installation.....	22
3.1.2 Filter backwash.....	23
3.1.3 Chemicals .....	23
3.1.4 Sampling and analysis .....	24
3.2 Baseline experiments in RSFs of Katwijk .....	24
3.3 Overview of pilot experiments .....	25
3.3.1 Validation of the pilot – tracer test.....	25
3.3.2 Dosage optimization.....	25
3.3.3 Influence of different top layer material.....	26
3.3.4 Variation of superficial filtration velocity .....	26

3.3.5 Backwash water settling velocity.....	27
4. Results & Discussion.....	28
4.1 Tracer test.....	28
4.2 RSF and Pilot without any doses.....	29
4.2.1 As results.....	29
4.2.2 Fe, Mn removal, nitrification and denitrification.....	30
4.3 Optimization of the chemical doses.....	32
4.4 Effect of filter media and filtration velocity.....	33
4.5 Pressure losses.....	36
4.5.1 Pressure losses caused by changing filtration velocity.....	36
4.5.2 Pressure losses as function of filter media.....	37
4.6 Runtime.....	39
4.7 Backwash water settling tests.....	42
5. Conclusions and recommendations.....	45
5.1 Conclusions.....	45
5.2 Recommendation for the application at Katwijk.....	46
5.2.1 Pilot results.....	46
5.2.2 Differences between the pilot filter and the filters in Katwijk.....	46
5.2.3 Additional research.....	47
References.....	48
Appendice A: Water quality parameters pilot compared to RSFs Katwijk.....	50
Appendice B: Lindquist diagrams at 4, 6, 10 m/h.....	51
Appendice C: Backwash experiment, samples after 2 minutes of backwashing.....	54
Appendice D: Proposal Jar tests for the influence of PAC on effectiveness of MnO <sub>4</sub> and Fe(III) .....	55

# 1. Introduction

## 1.1 Arsenic in drinking water in the Netherlands

The removal of arsenic (As) from drinking water is currently an active research area in the Netherlands. The World Health Organization (WHO) guideline for As in drinking water is 10 µg/l, which coincides with the national standard in the Netherlands. However, most drinking water companies in the Netherlands use a company limit of 5 µg/l. The WHO guideline for As has been based on previously available As detection limits and removal technologies and the WHO suggests that if possible As should be removed from water as much as possible (Van Halem et al., 2009, WHO, 2011).

However, due to improved analytical methods it is nowadays possible to detect As at much lower concentrations. New treatment possibilities have also arisen and show a potential of realistically reducing the As concentration to levels <1 µg/l. Van de Wens et al. (2016), Ahmad et al. (2014), Ahmad et al. (2017b) reported that removal of As to <1 µg/L will be beneficial for human health and may as well be economically beneficial in the Netherlands. Thus, the association of drinking water companies in the Netherlands (Vereniging van waterbedrijven in Nederland (VEWIN) in Dutch) has recently recommended the drinking water companies in the Netherlands to aim at producing drinking water with <1 µg/l As. According to Ahmad et al. (2015) 28 drinking water treatment plants (DWTPs) produced drinking water with >1 µg/l As in 2013 and therefore require an upgrade.

## 1.2 Arsenic in drinking water at WTP Katwijk and its source

WTP Katwijk is one of the three treatment locations of the drinking water company Dunea N.V. WTP Katwijk produces drinking water for the region around the city of Leiden. The raw water source is the dammed-up Meuse and subsequent natural recharge of the dunes.

In Table 1 the As concentration during the treatment process is shown. It is clear that the majority of As at Katwijk is mobilized during the dune infiltration, up to a concentration of 3.6 µg/L (Dunea, 2016). In this study the focus is on the removal of As during treatment after dune infiltration and the dune effluent will be considered the “raw water source”.

**Table 1: As during drinking water production from source to plant effluent at WTP Katwijk (Dunea, 2016).**

Location	As (µg/l)
Dammed up Meuse	1.2
Inlet Brakel	1.0
Influent Dunes	0.8
Dune effluent	3.6
Drinking water	2.4

### 1.2.1 Treatment of dune effluent at DWTP Katwijk

The source water from the Meuse is pre-treated and then infiltrated into the dunes where the residence time is approximately 60 days. After abstraction, 2 mg /l powdered activated carbon (PAC) is dosed to the dune effluent. The water is then aerated by the use of two lanes of cascades. About 50% of the water is subsequently softened by the use of two pellet reactors, while the remaining water is bypassed and combined with the softening effluent. The mixed

water is treated by 20 rapid sand filters (RSFs) that operate at an average filtration rate of 4 m/h. As a final polishing step, the effluent of the RSFs passes through slow sand filtration (SSF) at an average filtration velocity of 0.30 m/h.

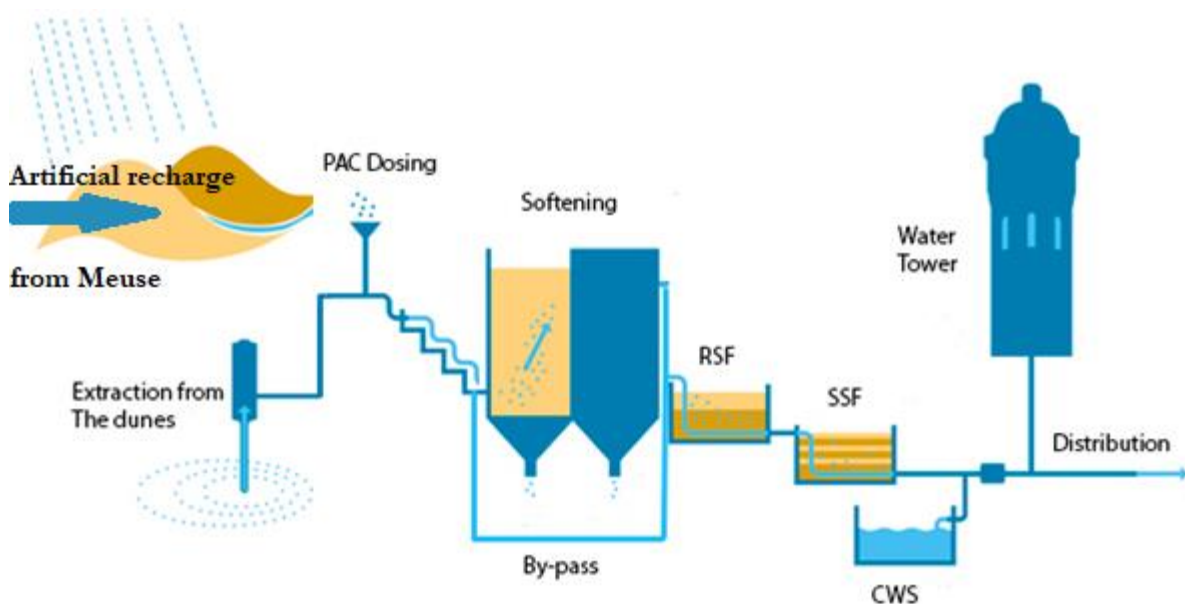


Figure 1: Drinking water production from source to plant effluent at WTP Katwijk (adapted from [www.dunea.nl](http://www.dunea.nl))

### 1.2.2 Dune infiltration

Dunea uses water stored in the dunes as a source for drinking water supply. Water stored in the dunes has slowly infiltrated through the dunes and is stored in aquifers underneath. Due to the higher demands, natural recharge by precipitation is insufficient. Therefore Dunea infiltrates pretreated dammed Meuse water into the dunes by infiltration ponds. The residence time of this infiltrated water is about 60 days, this ensures sufficient residence time for biological removal processes to take place. The dune infiltration currently contributes to the microbiological stability by providing a removal of pathogenic bacteria and viruses by 8 log units.

For Dunea the dunes also function as a buffer which ensures the water quality of the water that enters the treatment plant is relatively constant. Also the dunes provide a storage function, ensuring that even when the intake at the Meuse has to be closed (due to calamities with pesticides etc.) sufficient amount of water is available for the production of drinking water.

### 1.2.3 Powdered Activated Carbon dosage

At DWTP Katwijk 2 mg/l PAC is dosed in the dune effluent. The PAC is dosed periodically; every minute there are three injections of PAC. This dosing regime causes high peak concentrations of PAC. The dosing is applied in the cascades, well before the RSFs. Therefore, the dosed PAC forms a top layer on the surface of RSFs which ensures sufficient contact time for PAC to remove mostly taste and odor from the water.

### 1.2.4 Cascade Aeration

After the 60 day residence in the dunes, the water becomes anoxic with an average DO concentration of 3.1 mg/l, characterized by presence of manganese (Mn), iron (Fe) and even some ammonium ( $\text{NH}_4^+$ ). These compounds need to be removed for drinking water purposes. To increase the oxygen concentration (DO) and therefore oxidize these compounds and to remove some  $\text{CO}_2$  present in the water; cascade aeration is used.

### **1.2.5 Pellet softening**

Pellet softening is used to soften the water to prevent the precipitation of calcium carbonate at customers' washing machines etc. The DWTP has five pellet reactors of which two are always in use while others are used when maintenance is performed on the first two. In these reactors NaOH is used as a base chemical to increase the pH of the water and therefore cause oversaturation of CaCO<sub>3</sub>. Garnet sand is used as a seeding material to function as a kernel for CaCO<sub>3</sub> crystallisation (de Moel et al., 2006). Only 50% of the water after dune infiltration is treated by pellet softening, the other half is bypassed and mixed with the softened water to reach a final hardness of about 1.5 mmol/l.

### **1.2.6 Rapid Sand Filtration**

The treatment plant consists of two lanes of RSFs, each consisting of 10 RSFs. Each RSF has a surface area of 40 m<sup>2</sup> and consists of 1 m of sand (0.8 - 1.3 mm) d10 – d90 with uniformity coefficient (uc) 1.3 and a top layer of 0.5 m anthracite (1.7 – 2.8 mm) d10 - d90 with uc 1.3. The RSFs are operated under constant head (supernatant water level) at about 1 m. This is established by the use of an automatic valve in the effluent of each filter. This valve is managed based on the pressure difference between the top and the bottom of the filter, when the resistance in the filter increases the valve opens up automatically to keep a constant supernatant level.

At DWTP Katwijk on average 3.000 m<sup>3</sup>/h water is produced, this results in an average filtration velocity of about 4 m/h. The RSFs in Katwijk are designed to treat water at a maximum filtration rate of 6 m/h.

### **1.2.7 Backwash water treatment**

RSFs in Katwijk are currently backwashed after 7 days. The capacity of the backwash water treatment at DWTP Katwijk is just sufficient for regular operation of all the 20 RSFs. The first step of the backwash treatment consists of two primary sedimentation basins. One of the basins is used at a time while the other is kept dry to reduce the volume of the sludge in the sedimentation basin. Approximately once every year the dry basin is emptied and the basins are alternated. After the primary settling, water is pumped into a secondary sedimentation tank. In each sedimentation tank 10 mg/l iron chloride (FeCl<sub>3</sub>) is dosed to enhance the sedimentation in each tank. After this secondary basin the water is transported to three infiltration compartments where the water infiltrates into the dunes close to the treatment plant. After infiltrating into the dunes the water is collected again and is reintroduced in the infiltration ponds used for the infiltration of pretreated Meuse water.

### **1.2.8 Slow sand filtration**

The final polishing step in the treatment is the slow sand filtration (SSF). Due to the microbial activity in the top layer of the SSF (schmutzdecke) this polishing step ensures the microbiological safety and stability of the water by removing some nutrients, pathogens, bacteria and viruses and therefore further preventing regrowth during distribution. Furthermore the SSF treatment also polishes the effluent by filtration of small particles.

## 1.3. Scope of this thesis

### 1.3.1 Objectives

The goal of this research is to find opportunities to reduce residual As concentrations in drinking water to below 1 µg/l, specifically for the case of Katwijk (Dunea). Previous research has indicated the potential of As adsorption onto iron flocs, as well as the potential of Advanced Oxidation Coagulation Filtration (AOCF) (an oxidant dosage followed by a coagulant dosage prior to the filtration step to enhance the As removal) (Siddiqui and Chaudhry, 2017, Bordoloi et al., 2013, Ahmad, 2017).

Therefore, the goal of this research was to explore the effectiveness combining  $\text{MnO}_4 - \text{FeCl}_3$  as AOCF method for the case of Katwijk. Particular attention was given to the effect of filtration velocity and top layer material on the run times of this technology, as this is important for the application in full scale treatment plants. In addition, the impact of  $\text{MnO}_4 - \text{FeCl}_3$  dosing on backwash water settling was investigated.

### 1.3.2 Research questions

To evaluate the robustness of the  $\text{MnO}_4 - \text{Fe(III)}$  dosing technique during the RSFs, different filtration velocities and different top layer materials were evaluated. In addition the settling behavior of backwash water produced during backwashing was assessed.

To reach conclusive answers for this, the following specific research questions are composed:

- How is As removed in the existing filtration processes of DWTP Katwijk?
- What dosing combination is optimal for the application of  $\text{MnO}_4 - \text{Fe(III)}$  for the reduction of residual As to <1 µg/l in Katwijk?
- What influence does the dosing have on the filtration performance (turbidity) of the RSFs in Katwijk?
- How does the chemical oxidant ( $\text{NaMnO}_4$ ) influence the biologically mediated removal processes (ammonia, manganese) in the RSFs?
- Is there any difference in removal efficiency between the use of an anthracite or pumice top layer?
- What top layer material provides the best runtime for RSFs of Katwijk while using the  $\text{MnO}_4 - \text{Fe(III)}$  dosing?
- Is there any difference in removal efficiency and runtime of the filters between the use of a filtration rate of 4/6/10 m/h?
- What influence does the dosing have on the settling rate of the produced backwash water?

### 1.3.3 Thesis content

- Chapter 2 covers a literature study regarding As and the removal of As by the use of AOCF.
- In chapter 3 the materials and methods that are used to answer the research questions are discussed. Experiments that are used to find answers to the research questions are explained in detail.
- In chapter 4 the results of all the experiments are presented and discussed in detail.
- In chapter 5 first all research questions are answered based on the results in chapter 4 and conclusions are drawn. Secondly the difficulties and problems that are present for a direct translation from pilot results to actual RSFs in Katwijk are discussed. Thirdly recommendations for the application of AOCF in the current process in Katwijk are posed. Finally some recommendations for further research considering the application of AOCF in Katwijk are proposed.

## 2. Literature Review

### 2.1 Arsenic speciation

As is a naturally occurring metalloid in the Earth's crust. It is estimated that in the upper layer of the earth the concentration of As is about 6 mg/kg of soil (Sevil, 2005, Smedley and Kinniburgh, 2001). As is often present in rock-forming minerals and is mostly bound to iron oxides (Dissanayake and Chandrajith, 1999). As mostly occurs in one of the following two oxidation states: +3 (As(III)) and +5 (As(V)), however oxidation states -3 and 0 also occur, but are not commonly found. As is more toxic in the As(III) form, the human body metabolizes As(III) quicker than As(V) and As(III) accumulates quickly in nails and hair (Sorlini and Gialdini, 2010). One of the most common symptoms of being exposed to drinking water with elevated As concentrations are skin diseases. These skin diseases can vary from relatively harmless pigmentation disorders to skin cancer but As poisoning can also lead to cancer, heart and kidney failure, diabetes and paralysis (Dissanayake and Chandrajith, 1999, Kersten and Vlasova, 2009).

In anoxic conditions As with an oxidation state of +3 prevails while in aerobic conditions As is mostly found in an oxidation state of +5 (Onireti et al., 2016). Due to the anoxic conditions in the deeper ground layers; reduction of Fe(III) to soluble Fe(II) occurs, furthermore, in these anoxic conditions As(III) prevails. As(III) has a lower affinity to adsorb to Fe(OH)<sub>3</sub> than As(V). Thus when the As(V) is reduced to As(III) it desorbs from the Fe and dissolves in water. This process is called the mobilization of As in water (WHO, 2001, WHO, 2011). As mobilization is also induced by microbiology, this is however estimated to be significantly less impactful compared to the reduction and desorption of As(V) (Bora et al., 2016).

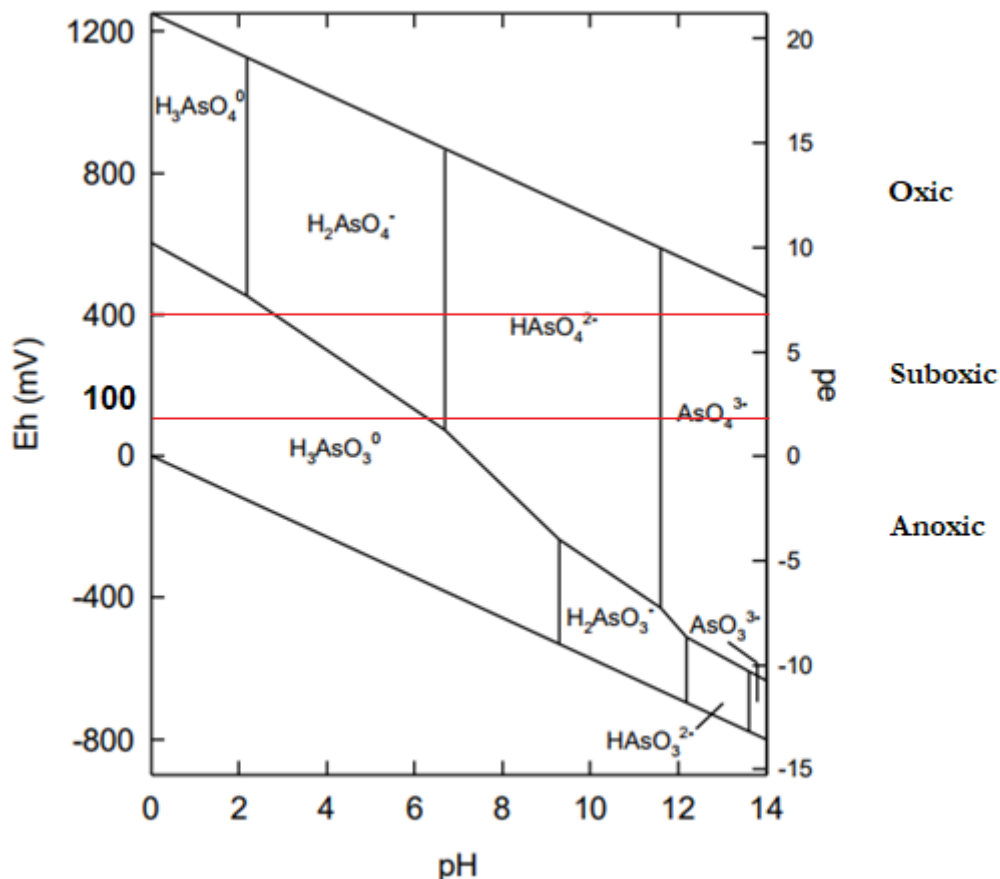


Figure 2: pH - Eh diagram of arsenic compounds (adapted from (Smedley and Kinniburgh, 2001))

As(III) can occur in three different forms. The form that it appears in depends on the pH of the environment and the redox potential. In Figure 2 the Eh – pH diagram of As is shown, in this diagram the speciation of As in different environments is presented.

In anoxic conditions (Eh <100 mV) As(III) can be found as  $\text{H}_2\text{AsO}_3^-$  with a  $\text{pK}_a$  of 9.1. At slightly higher pH it can be found as  $\text{HAsO}_3^{2-}$  with a  $\text{pK}_a$  of 12.1 and finally in water with even higher pH it can be found as  $\text{AsO}_3^{3-}$  with a  $\text{pK}_a$  of 13.4 (Barringer and Reilly, 2013).

As(V) is dominant in oxic conditions (Eh > 400 mV) and can also occur in three different states based on the pH of the environment. Depending on pH As(V) is in the form of  $\text{H}_3\text{AsO}_4$ ,  $\text{H}_2\text{AsO}_4^-$  and  $\text{HAsO}_4^{2-}$  with a  $\text{pK}_a$  of respectively 2.1, 6.7 and 11.2 (Barringer and Reilly, 2013).

## 2.2 Previous research: iron dosing in Katwijk

In a previous study done by Dunea the effect of Fe(III) dosing in the influent of RSFs was tested. In this experiment 0.25 mg Fe(III)/l was dosed in the influent of the RSFs in Katwijk. In this experiment it was found that when dosing 0.25mg Fe/l the As removal during rapid sand filtration doubled. This meant that in the effluent of the RSFs the As concentration decreased from about 3.5  $\mu\text{g}/\text{l}$  to around 2.3  $\mu\text{g}/\text{l}$ . Without dosing any Fe(III) the As concentration decreased to about 2.9  $\mu\text{g}/\text{l}$  during the rapid sand filtration process (Dunea, 2011).

During the Fe(III) dosing study executed in 2011 the total iron content was on average about 0.5 mg/l and the average As in the effluent was about 2.3  $\mu\text{g}/\text{l}$ .

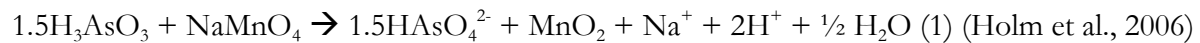
## 2.3 Advanced Oxidation Coagulation Filtration (AOCF)

AOCF is a technique based on two different processes. The first process is the oxidation of a compound by dosing strong oxidants. The second process is the coagulation. These chemicals are dosed to improve the formation of flocs. These flocs are then removed by the filtration step afterwards.

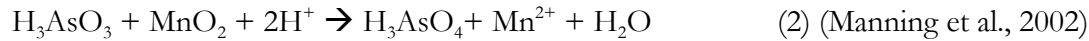
### 2.3.1 Different oxidants

As(III) does not bind as well to flocs as As(V) and therefore it is first oxidized to As(V). Multiple different oxidants are available for the oxidation of As(III). Sorlini and Gialdini (2010) compared the As(III) oxidation by different commonly used oxidants. In this research hypochlorite, permanganate, chlorine dioxide and monochloramine were compared. Each oxidant was tested when dosed at a stoichiometric ratio (R) of 1 and 3. R = 1 means that in theory exactly enough oxidant is dosed to oxidize all the As(III), R = 3 meaning that 3 times as much is dosed. Samples were taken until 50 hours had passed. In the research it was found that both monochloramine and chlorine dioxide did not fully oxidize all the As(III) (even at R=3) within 50 hours. Hypochlorite and permanganate both perform very well. Hypochlorite oxidizes about 85-92% of all the As(III) within 30s of contact time. Permanganate shows the quickest reaction times with oxidation yields of about 95% at R=1 after a reaction time of 7s (Sorlini and Gialdini, 2010).

The oxidation of As(III) to As(V) by  $\text{MnO}_4^-$  occurs following two reactions:



And



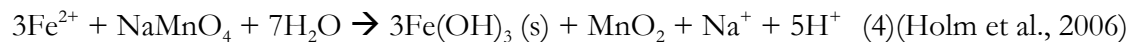
Reaction 1 shows that the As is oxidized by the  $\text{NaMnO}_4^-$ , in this process  $\text{MnO}_2$  is formed,  $\text{MnO}_2$  contributes slowly in the removal of As.  $\text{MnO}_2$  can oxidize some As itself following reaction 2, this reaction is however quite slow compared to the oxidation by  $\text{MnO}_4^-$  (Li et al., 2007). Following the reaction stoichiometry of both reactions it is found that about 5 moles of As(III) can be oxidized by 2 moles of  $\text{MnO}_4^-$  (Li et al., 2007).

### 2.3.2 Different coagulants

For As adsorption aluminum oxides are proven to be not very effective while iron hydroxides are proven to be effective (Ahmad, 2014, Kersten and Vlasova, 2009, Chen et al., 2007). The coagulant ( $\text{FeCl}_3$ ) forms iron-oxides which bind to the As(V), the flocs that are then formed are removed by the RSFs. The iron hydroxides are formed according to the following reaction:



Iron hydroxides ( $\text{Fe}(\text{OH})_3 (\text{s})$ ) are formed,  $\text{HAsO}_4^{2-}$  has an affinity to bind to the OH sides of the  $\text{Fe}(\text{OH})_3$ . Fe(III) is chosen over Fe(II) as the coagulant due to the fact that any form of Fe(II) like  $\text{FeSO}_4$  first has to be oxidized before it forms iron hydroxides which adsorb As. This would then consume some of the oxidant which was required for As(III) oxidation. The oxidation of  $\text{Fe}^{2+}$  and production of iron oxides occurs according to the following reaction:



As can be seen in reaction 4  $\text{NaMnO}_4^-$  can be consumed by the  $\text{Fe}^{2+}$ , not all of the  $\text{Fe}^{2+}$  will be oxidized by the  $\text{NaMnO}_4^-$  also some oxidation due to the available  $\text{O}_2$  will occur. At neutral pH the redox potential of the  $\text{Fe}(\text{II}) \leftrightarrow \text{Fe}(\text{III})$  is higher than the potential of  $\text{As}(\text{III}) \leftrightarrow \text{As}(\text{V})$ , this means that Fe(II) will be prioritized for oxidation.

## 2.4 Rapid Sand Filtration (RSF)

Runtimes and pressure build up are important parameters of the RSFs for the applicability of the AOCF process in the DWTP at Katwijk. By dosing extra chemicals (mostly Fe), the filterbed is more heavily loaded which influences the clogging and thus breakthrough and resistance in the filter.

Filtration of particles occurs through different mechanisms. Some of these mechanisms are: Sedimentation, interception, diffusion, inertia and turbulence (TuDelft, 2017).

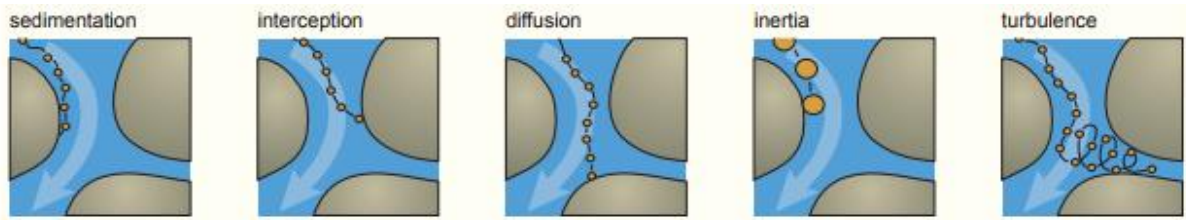


Figure 3: Filtration mechanisms(TuDelft, 2017)

These mechanisms of filtration all cause an accumulation of particles in the pores between the filter media and start to clog the filter. Due to the clogging of the filter the velocity of the water has to increase (to satisfy the constant flow). Filter resistance is directly correlated to the flow velocity. This relation is described by the Carman-Kozeny equation:

$$\frac{H_0}{L} = 180 * \frac{v}{g} * \frac{(1 - p_0)^2}{p_0^3} * \frac{v}{d_0^2}$$

When expressed over the runtime of a filter the Carman-Kozeny equation can be displayed in a Lindquist diagram. In the Lindquist diagram the amount of resistance in a specific part of the filter can quickly be seen. Figure 4 shows an example of a Lindquist diagram of a single media filter (TuDelft, 2017). The red line in the figure displays the hydrostatic line, the purple (t=0 hours) shows the clean bed resistance and the other lines show the resistance over time. The more the lines diverge from the purple line, the more resistance is in that particular part of the filter. Because the filters clog more in the top layer (and therefore produce more resistance), the lines diverge more from the purple t=0 hours line.

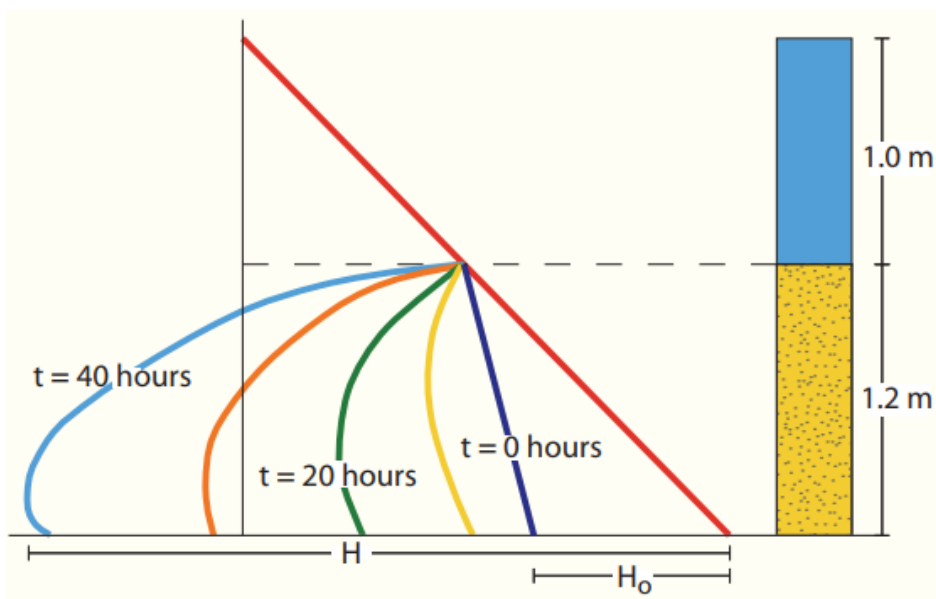


Figure 4: Example of a Lindquist diagram of a single media filter (TuDelft, 2017)

In the case of multi-layer filtration the expected Lindquist diagram is different. Due to the difference in grain size each layer filters different particles. The coarser top layer removes the big particles from the water while the small particles in the water move through this layer. These smaller particles are however removed by the finer bottom layer in the filter. This causes that both layers of the filter participate in the filtration of water. The different grain sizes also cause the distribution of the particles to be spread more evenly. Figure 5 shows the Lindquist diagram expected for a multi-layer filter that functions well. As can be seen the top part of each layer is

mostly clogged (and causes resistance). A well-functioning multi-layer filter produces less resistance than a single layer filter and therefore has a longer runtime.

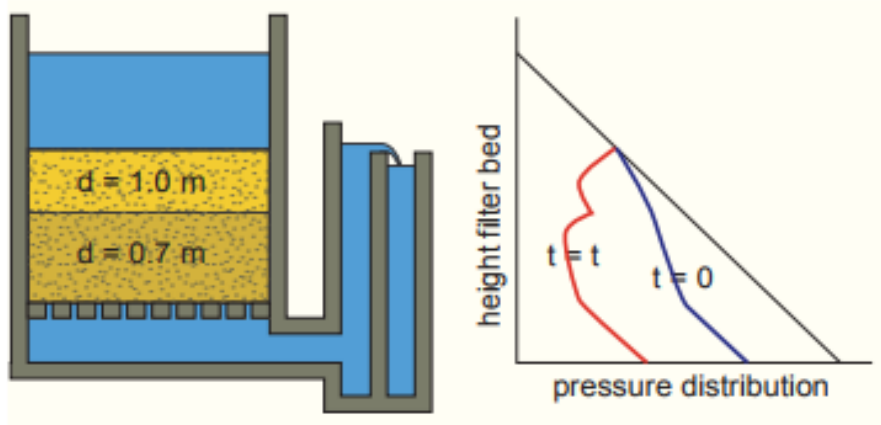


Figure 5: Lindquist diagram of a multi-layer filter (TuDelft, 2017)

For a filter to perform well there are some requirements that need to be satisfied. Based on pilot studies on 200+ pilot filters, the ratio  $L/d_{10}$  should be  $>1000$  for multi-layer filters (Kawamura, 1999). Furthermore the settling velocity of the grains is important for the backwashing of the filter. If the proportion between the two filter media used is not correct; loss of filter media or insufficient cleaning can be expected. Finally the uniformity of the filter media is very important. The uniformity coefficient,  $uc$  ( $uc = D_{60}/D_{10}$ ) should be sufficiently low to minimize the mixing of the two filter media. (Kawamura, 1999) states that an  $uc$  of  $<1.4$  suffices for well-designed filters.

## 2.5 Previous AOCF research at Dunea on As removal

### 2.5.1 AOCF Jar Tests

Dunea performed jar tests to find the effectiveness of AOCF for the treatment plant of Katwijk. Dunea had previously executed research on As removal by dosing  $\text{FeCl}_3$  in RSF influent and found a considerable decrease in arsenic, however also a considerable decrease in runtime of the RSF. Based on these results combined with the results achieved in Dorst (Ahmad et al., 2014) jar test experiments were designed and executed (Ahmad, 2017).

Three different experiments were executed:

- Dosing only  $\text{KMnO}_4$  in RSF influent
- Dosing only  $\text{FeCl}_3$  in RSF influent
- Dosing both  $\text{KMnO}_4$  (first) and  $\text{FeCl}_3$  (second) in RSF influent

All experiments were executed in Katwijk using a jar test device with continuous mixing.

The results of just dosing  $\text{KMnO}_4$  did not satisfy the desired residual As concentration of  $<1\mu\text{g/l}$ . Even at higher doses the concentration of As did not decrease any further; from this it can be concluded that the As removal is limited by the availability of adsorption sites.

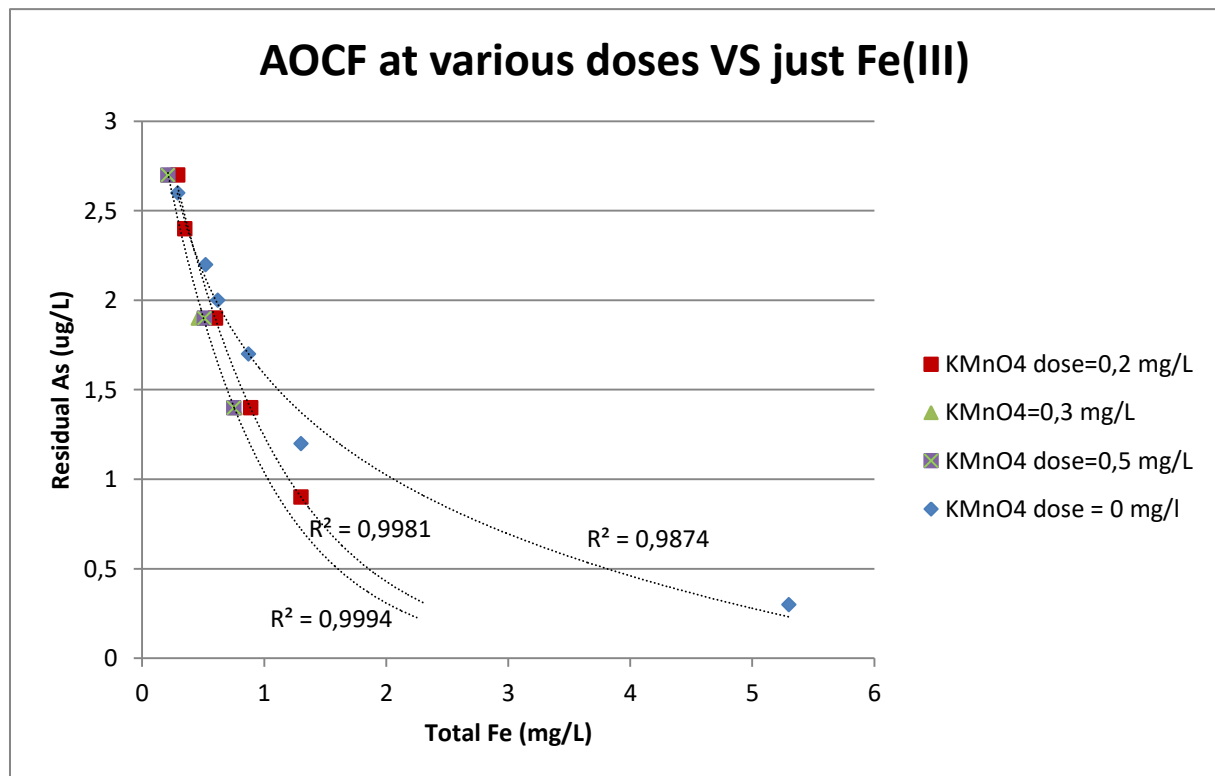


Figure 6: AOCF jar test results (Ahmad et al., 2017b)

As can be seen in Figure 6 when dosing just Fe(III) in the water a total Fe(III) concentration of 2.0 mg/l is required. The initial Fe(III) concentration in the RSF influent is about 0.3 mg/l so to reduce the As concentration to  $<1\mu\text{g/l}$  a Fe(III) dose of about 1.7 mg/l is required.

Figure 6 also shows that when AOCF is applied, the amount of Fe(III) required also decreases. At a  $\text{KMnO}_4$  dose of  $>0.3$  mg/l the required Fe(III) dose did not decrease any further and the lines for 0.3 and 0.5 mg  $\text{KMnO}_4$  coincide, at these doses all the As(III) was being oxidized to As(V) within the available contact time. Based on these results the optimal doses of  $\text{KMnO}_4$  and Fe(III) were set at respectively 0.3 and 0.7 mg/l.

### **2.5.2 Construction of the AOCF pilot filter**

In 2016 Dunea started with the setup of pilot experiments. Due to the biological activity in RSFs a pilot requires sufficient runtime to start producing results comparable to the RSFs in Katwijk. This was necessary before any additional experiments could be executed. The pilot produced comparable results after about one month of runtime (3 backwash cycles), both nitrification and manganese removal appeared to be fully functional (Dunea, 2016).

First AOCF experiments were executed with doses of 0.4 mg  $\text{NaMnO}_4$  /l and 0.7 mg  $\text{FeCl}_3$  /l (achieved from jar tests(Ahmad et al., 2017b)). The results of these experiments however did not satisfy the boundary condition of a residual As concentration of  $<1 \mu\text{g/l}$ .

During the internship it was found that the runtimes of the RSFs in Katwijk were much shorter than what was found in the pilot filter. After inspection of the top layer of the RSFs in Katwijk this difference was attributed to the occurrence of mudballs.

Turbidity of the effluent was found to decrease by a factor 10, from 0.1 – 0.2 to about 0.01-0.02 until breakthrough was reached after approximately 8 days (Dunea, 2016).

### 3. Materials and methods

#### 3.1 Pilot setup

##### 3.1.1 Pilot installation

Pilot experiments were performed at WTP Katwijk with a pilot installation built at KWR. The setup consisted of two stainless steel columns with an effective filter height of 2.25 m and a total height of 2.5 m. The column diameter was 0.25 m, which should be sufficient to neglect the wall effects in the column. A rule of thumb that is used to ensure no significant wall effects are found is that the ratio between diameter of the column and the diameter of the filter media should be about 20-30 (EPA, 2015). Applying a ratio of 30 this means that the biggest allowed filter media grains are 8.3mm.

Each column is filled with a different filter composition. Both filters contain a bottom layer of 1m sand (0.8-1.3mm) with a uc of 1.3. The anthracite filter contains 0.5m anthracite with a grain size range of (1.6 – 2.5mm) while the pumice filter contains 0.5m of pumice with a grain size range of (2.5 - 3.5mm).

Both columns were fed with the mixture of cascade effluent and softened water from DWTP Katwijk, buffered a 1000 l tank, during regular operation the water in the tank had a residence time of 2.5h. This tank was filled with RSF influent water. This water is a combination of softened water and bypass water. The tank overflowed to ensure a stable water quality to the columns. Each column had a separate inflow pump that pumped in water from the buffer. The normal flow rate that was used was 200 l/h per column which resulted in a filtration rate of 4 m/h through each column.

A second buffer tank was used to store the filtrate from both the columns. This stored clean water was then used for backwashing the pilot filters. During backwashing, flow of 3000 l/h was applied which corresponds to backwash velocities of 60 m/h; similar to what is used at DWTP Katwijk.

For the holding chemicals (solutions of NaMnO<sub>4</sub> and Fe(III)) four tanks of 60 l each were used. Four peristaltic pumps were used to pump the chemicals into the columns at a steady rate.

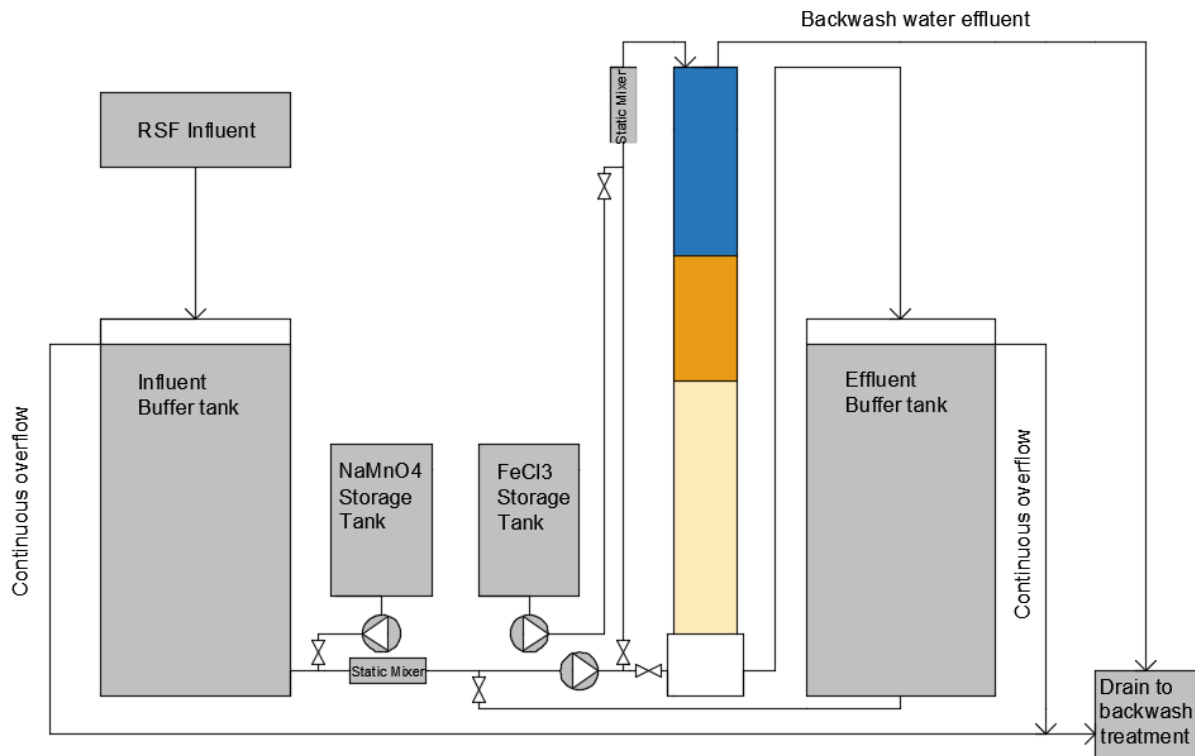


Figure 7: Schematic of pilot installation used in this study.

### 3.1.2 Filter backwash

To ensure the integrity of the results obtained in the pilot filters, the backwash of the filters was closely observed making sure there was no washing out of filter material. Each new experiment is started with a clean filter to ensure that representative data is obtained. Not sufficiently cleaned filters will clog faster due to some leftover particles being trapped in the filter. This causes shorter runtimes than when the bed is fully cleaned and thus skews the results. Too much cleaning with too high flow velocities may also cause problems. The high velocities can potentially wash filter media out of the column, lowering the effectiveness of the filter. Another possibility of too high backwash velocities is the removal of the iron- and or manganese coating on the filter material. During the ripening and operation of the filter Fe- and Mn- oxides have deposited on the filter media forming a coating on the filter material. These oxides are an important part of the As removal process and are therefore very important to not disturb.

To simulate full-scale conditions and to ensure sufficient cleaning the backwash regime that is used at WTP Katwijk was used in the pilot experiments.

Table 2: Backwash regime used in pilot experiments.

Step		Velocity (m/h)	Duration (min)
1	Drain supernatant water until 10cm water is left on top of the filter		
2	Air scour	55	10
3	2 minutes of pause to remove some leftover air bubbles stuck in the filter bed.		
4	Backwash with water	60	10

### 3.1.3 Chemicals

Chemicals were prepared by the use of 40% stock solutions provided by HWL (Het Waterlaboratorium in Dutch). The chemicals were manually further diluted by the use of tap water. In the storage tank the  $\text{NaMnO}_4$  was diluted to 2 mmol  $\text{MnO}_4^-/\text{l}$  (0.25 g  $\text{NaMnO}_4/\text{l}$ ).  $\text{FeCl}_3$

is diluted to 5 mmol Fe(III) /l (0.3 g FeCl<sub>3</sub>/l). The solutions were prepared once every week and were stirred 2 times per day.

### 3.1.4 Sampling and analysis

Samples were manually collected and sent for analysis to HWL. Before the collection of a sample the taps were opened for half a minute at constant flow to ensure a representative sample. pH, dissolved oxygen (DO), and Temperature were measured on site by a hand-held (Hach HQ40D). Turbidity was measured by hand held device (Hach 2100P ISO Turbidimeter). Turbidity of the effluent of both the columns was also constantly measured and logged by the use of online turbidity meters.

In most cases unfiltered and 0.45 µm filtered samples were collected and analyzed for As, Fe and Mn. Filtration of the samples was done by filtration through 0.45 µm disk filters prior to being sent for analysis. The analysis of metals was done by the use of ICP-MS (Inductively coupled plasma mass spectrometry) and results were reported usually within a week.

As speciation was performed by the use of the method proposed by (Clifford et al., 2004) by the use of an ion exchange resin. The water sample was first filtered through a 0.45 µm filter and followed by filtration through the ion exchange resin. The resin exchanged As(V) with Cl, while As(III) remained present in the filtrate.



Figure 8a: Hach Multimeter

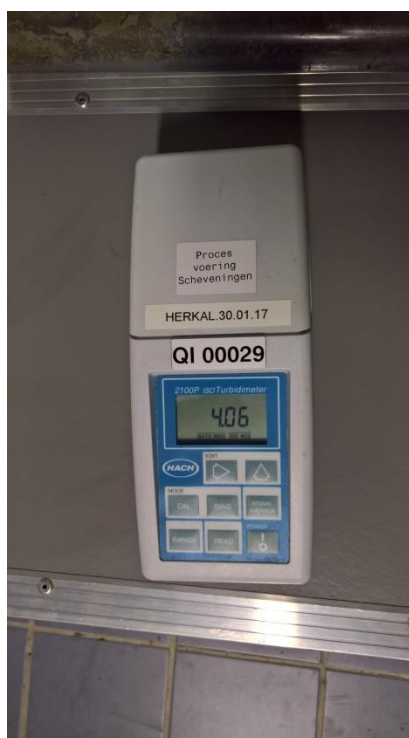


Figure 8b: portable turbidity meter

### 3.2 Baseline experiments in RSFs of Katwijk

The translation of the results found in the pilot to the application on full scale is difficult. To make the translation as easy as possible it is important to compare the functioning of the full scale RSFs to the functioning of the pilot installation. Therefore, before the addition of any chemicals, multiple samples over the filter height were taken to analyze the functioning of the filter. These samples are analyzed for turbidity, nitrate, unfiltered and filtered iron, manganese, As and finally As speciation. These results are compared to the results of the same experiment in the pilot installation.

### 3.3 Overview of pilot experiments

Based on the jar tests performed in Katwijk (Ahmad, 2017) a series of pilot experiments were performed. The pilot experiments were designed to answer the research questions concerning the effectiveness of the  $\text{MnO}_4 - \text{Fe(III)}$  dosing and the effects of top layer material and filtration velocity on this efficiency.

To answer the research questions posed before; multiple different dosing and filtration settings were used in the pilot. Settings varied based on filtration velocity, grain size of the material in the top layer and finally different dosing concentrations.

**Table 3: Experiments performed and important parameters**

Experiment	Adjusted parameters	Investigated parameter
Validation/tracer test	Conductivity ( $\mu\text{S/m}$ )	Residence time (min)
Dosage optimization	Fe(III) dosage (mg/l)	As concentration ( $\mu\text{g/l}$ )
	NaMnO <sub>4</sub> dosage (mg/l)	
Influence top layer	Anthracite (1.6 – 2.5 mm)	Runtime (d)
	Pumice (2.5 – 3.5 mm)	As concentration ( $\mu\text{g/l}$ )
Filtration velocity	4 m/h	Runtime (d)
	6 m/h	As concentration ( $\mu\text{g/l}$ )
	10 m/h	
Backwash	No AOCF (current situation)	Settling velocity (m/h)
	AOCF applied	

#### 3.3.1 Validation of the pilot – tracer test

To verify the usefulness of the results achieved in the pilot; the pilot has to be validated. To validate the pilot installation a tracer test was executed. This tracer test was necessary to see if the results acquired in the pilot installation were representative for the full scale situation and that there are no preferred flow paths along the edges of the column. A high concentration salt solution was dosed directly at the top of the filter bed (5cm above the top of the filter bed). The measured travel time between the top of the filter bed and the effluent is compared to the theoretical expected time based on the filtration velocity and porosity of the filter. The tracer test was performed twice, once in a clean bed right after backwashing and once at a filter runtime of 48 hours. This is preferred to make sure there is no substantial change in flow patterns over time.

#### 3.3.2 Dosage optimization

Starting dosages were found based on jar tests performed in a previous research (Ahmad et al., 2017b). Jar test conditions are however vastly different from full scale conditions. Mixing properties and contact time are two parameters that strongly influence the effectiveness of the oxidation and flocculation.

Different dosages are applied to find the minimum that is necessary to reduce the As concentration to  $<1 \mu\text{g/l}$ . The effectiveness of these doses is compared between the two filters. Not only the removal of As was measured, also other parameters that define the filtration performance (turbidity, runtime, ammonia removal, manganese removal) are compared. The dosing that is used at the start is the dosage found in the jar tests earlier performed (Ahmad et al., 2017b). These dosages (0.5mg/l NaMnO<sub>4</sub> and 1.0 mg /l Fe(III)) were used as a baseline to start with. Four alternative settings were applied on both filters to find the optimal dosage required to reduce residual As to below  $<1\mu\text{g/l}$ . To find the filter performance the turbidity, pressure loss, residual iron & manganese and finally breakthrough time are also measured. All the different parameters are measured for both filters to provide an adequate comparison.

To find the most optimal dosage to reduce the As to  $<1 \mu\text{g/l}$  both the  $\text{NaMnO}_4$  and  $\text{FeCl}_3$  dosages were adjusted. The following settings were used:

**Table 4: Dosing optimization experiment**

Setting	$\text{NaMnO}_4$ dosage (mg/l)	Fe(III) dosage (mg/l)
1	0.5	1.0
2	0.25	1.0
3	0	1.0
4	0	0.7
5	0.4	0

The first set of experiments were focused on the reduction of the usage of  $\text{NaMnO}_4$  as the jar test performed in Ahmad et al. (2017b) showed that a  $\text{KMnO}_4$  dose of 0.3 mg/l showed similar results as a dose of 0.5 mg/l. Finally the effect of a lower dosage of iron is assessed, as the iron dosage plays the biggest role in the additional clogging of the filters and is thus very important to be dosed as little as possible.

### 3.3.3 Influence of different top layer material

The pilot setup provides two filters that use the same influent. This setup is thus perfect to use for the comparison of two types of filter media. In each filter a different top layer was used, while the bottom layer comprised of exactly the same type of material and grain size. The difference in top layer was caused by the use of Anthracite in the first filter while using Pumice in the second filter. The first filter contained a 1 m bottom layer of sand (0.8 mm – 1.3 mm) and a 0.5 m top layer of anthracite (1.7 mm – 2.8 mm). The second filter contained a 1m bottom layer of sand (0.8 mm - 1.3 mm) and a 0.5 m top layer of pumice (2.5mm – 3.6mm). The bottom layer in both the filters was identical to make sure the differences in the filter can only be attributed to the difference in top layer. Pumice is chosen for comparison due to the high grain size and therefore the porosity of the top layer. This pumice top layer is currently also used in another treatment plant of Dunea (Scheveningen).

### 3.3.4 Variation of superficial filtration velocity

The other parameter that was studied was the filtration velocity, experiments with varying filtration velocity were performed. When filters were subjected to higher filtration velocities it is expected that the effluent quality will decrease. Our hypothesis was that if the filtration velocity increases; the iron flocs that are formed will penetrate deeper into the filter bed and will not be removed by cake filtration at the top layer of the filter bed. This prevents the top layer from clogging extremely fast and will ensure a better distribution of particles in the filter bed. The risk in using a higher filtration velocity is the shorter contact time between the As in the water and the iron flocs. This could potentially decrease the effectiveness of the As removal and thus cause a higher filtrate As

In the experiments with varying superficial filtration velocity three different settings are used. The first setting, the baseline of 4 m/h, 6 m/h (the maximum applied during peaks) and finally 10 m/h (a setting that is not applied in Katwijk but is taken into account in this research as an extreme).

All experiments were performed with dosages of 0.5 mg  $\text{NaMnO}_4$  /l and 1.0 mg Fe(III) /l. Every setting was tested for 3 runtimes to reach equilibrium; the first runtime was never sampled as equilibrium may not be reached within one runtime.

### **3.3.5 Backwash water settling velocity**

Due to the changes in the treatment process and thus the removal properties of the RSF the composition of the backwash water may also change. Due to the addition of iron the top layer will clog quicker and the particles will not penetrate as deep into the bed. The iron dosage also likely causes the appearance of bigger flocs, these flocs have a higher settling rate than the small light flocs. Due to these changes in settling velocity it is possible that the backwash water treatment facility can be run in a different way. To investigate if any differences in settling properties occur, a small experiment was performed during the backwashing the filters. These small settling experiments were done with and without the addition of 0.5 mg/l  $\text{MnO}_4$  and 1.0 mg/l Fe(III).

At the end of a filter runtime when the filter was backwashed two 1l samples were taken after 1 and 2 minutes. The samples were stored in two 1.5l measuring cylinders. Every 5 minutes the location of the clear divide between clear water and turbid water (from now on in this thesis referred to as sedimentation front) was noted. Additionally the turbidity was measured at 750ml.

Additionally secondary experiment was performed during a backwash of a RSF in Katwijk (without applying AOCF) and the backwash of the anthracite pilot filter. A mixed sample was made of the backwash by mixing water over the first 4 minutes. Every 5 minutes a picture was made of the sedimentation front to compare the settling properties.

## 4. Results & Discussion

### 4.1 Tracer test

The tracer test was executed to confirm the absence of preferred flow paths along the edge of the column. As can be seen in Figure 9 it is apparent that there was no short circuiting along the edge of the column. If short circuiting would occur it was expected that the conductivity change would occur much faster and less abrupt as was found in Figure 9. Based on calculations the orange lines were drawn, these lines represent the time when it was expected that the change in conductivity occurs. These lines were calculated based on the porosity (obtained from literature) of sand 0.4 and anthracite 0.5. As can be seen in the figure; these lines almost perfectly coincided with the measured increase in conductivity. Deviations from the expected lines can be explained by the transport mechanisms through porous material (Mau, 1992). Both advection and dispersion play a big role in the deviations. Another reason for the small deviations is assumption of the porosity of the filter material and not having exact measurements. Differences in expected porosity causes deviations in flow velocity through the pores and can therefore cause faster or slower breakthrough than expected.

The tracer test was performed in both the clean bed and in the 48 hours runtime test, this means that during the experiments the column remained consistent in flow patterns.

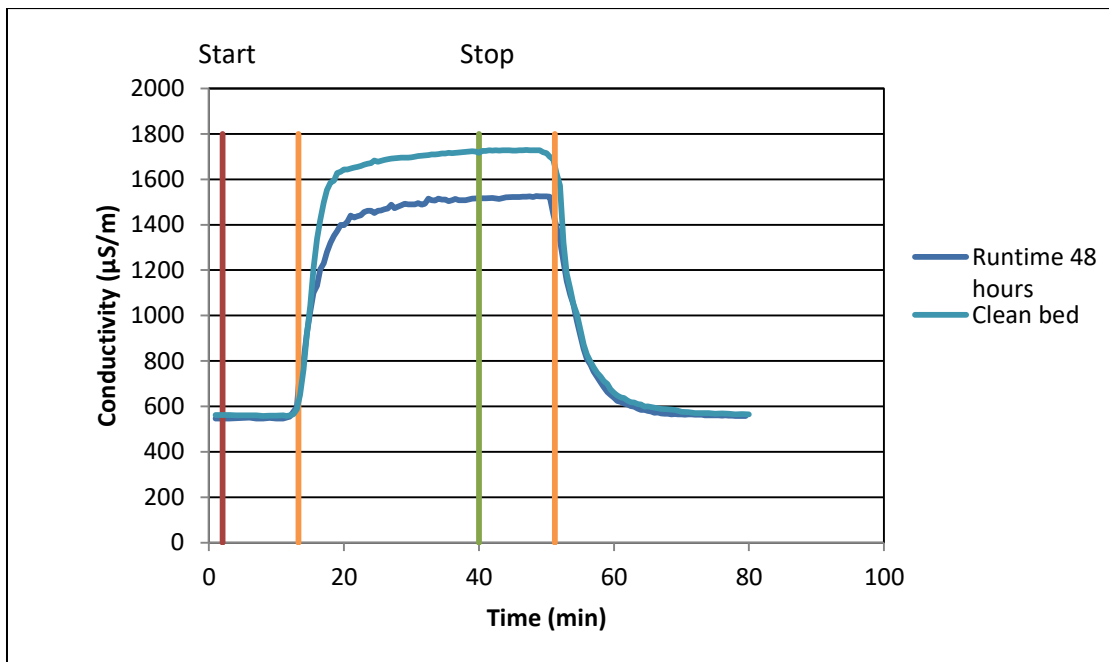


Figure 9: Tracer test. Red line is starting time of dosing, orange line is the expected arrival of the front. Green line dosing stopped

## 4.2 RSF and Pilot without any doses

### 4.2.1 As results

As can be seen in Figure 10 the As speciation changed after the RSF while the total concentration remained relatively constant. This means that As(III) was converted (chemically or biologically) to As(V) during RSF. In Figure 10 it is shown that the As(III) concentration rapidly decreased in the first 30 cm of the filter bed and then gradually decreased further deeper in the filter. At the same time the As(V) concentration increased over the height of the filter.

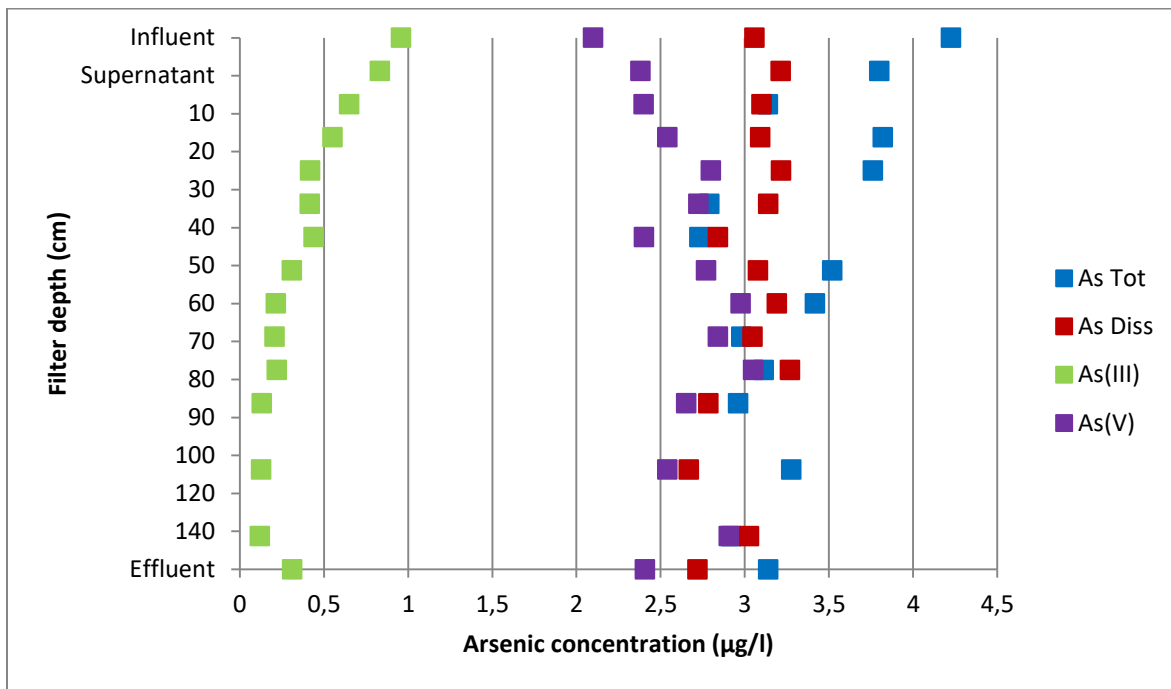


Figure 10: As speciation over the height of RSF 8A in Katwijk

After the ripening period of approximately 4 weeks, the As speciation over the height of the pilot filter showed similar patterns as RSF 8A in Katwijk. Figure 11 shows a steady decrease of As(III) and an increase in As(V) showing a clear conversion of As(III) to As(V).

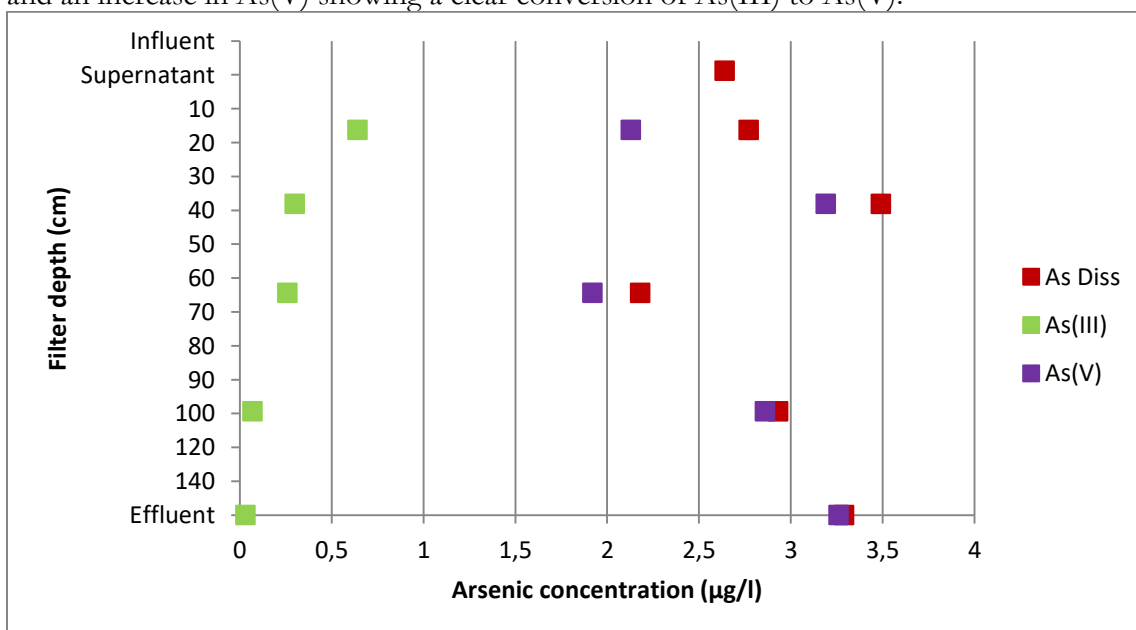


Figure 11: As speciation over the height of the anthracite pilot filter

#### 4.2.2 Fe, Mn removal, nitrification and denitrification

In Figure 12 the Fe and Mn removal over the height of the filter is shown. Mn was mostly removed in the top 30cm of the filter, decreasing from about 20 $\mu\text{g/l}$  to about 0.5 $\mu\text{g/l}$  after 30cm of RSF. Fe was also mostly removed in the top 30cm of the filter, however after 30cm the Fe concentration kept on decreasing until the bottom of the filter.

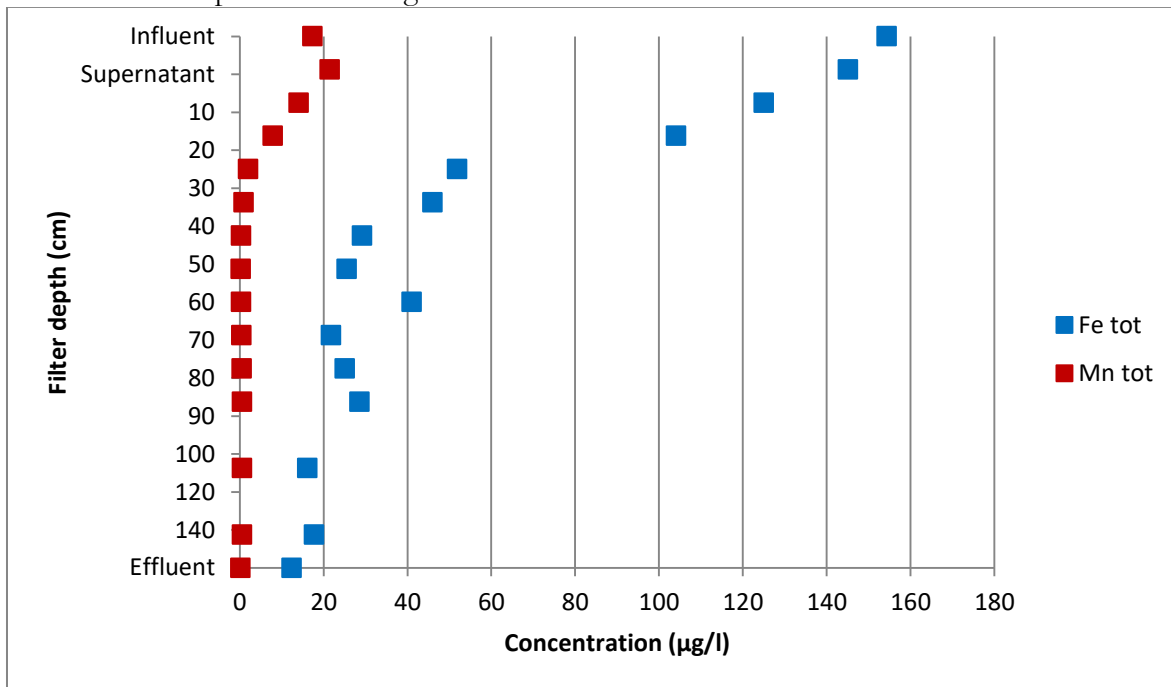


Figure 12: Fe and Mn removal over the filter height of RSF 8A in Katwijk

Figure 13 shows the behaviour of  $\text{NH}_4$ ,  $\text{NO}_2$  and phosphate. Total phosphate decreased rapidly in the first 20-30 cm from 0.065 mg/l to about 0.05 mg/l, this was most likely due to the removal of Fe in the same part of the RSF. Deeper into the filter bed the phosphate concentration remained relatively stable at 0.045 mg/l.

Ammonium concentration decreased mostly in the top 20 cm of the filter while nitrite decreased after 20cm and was fully converted to nitrate.

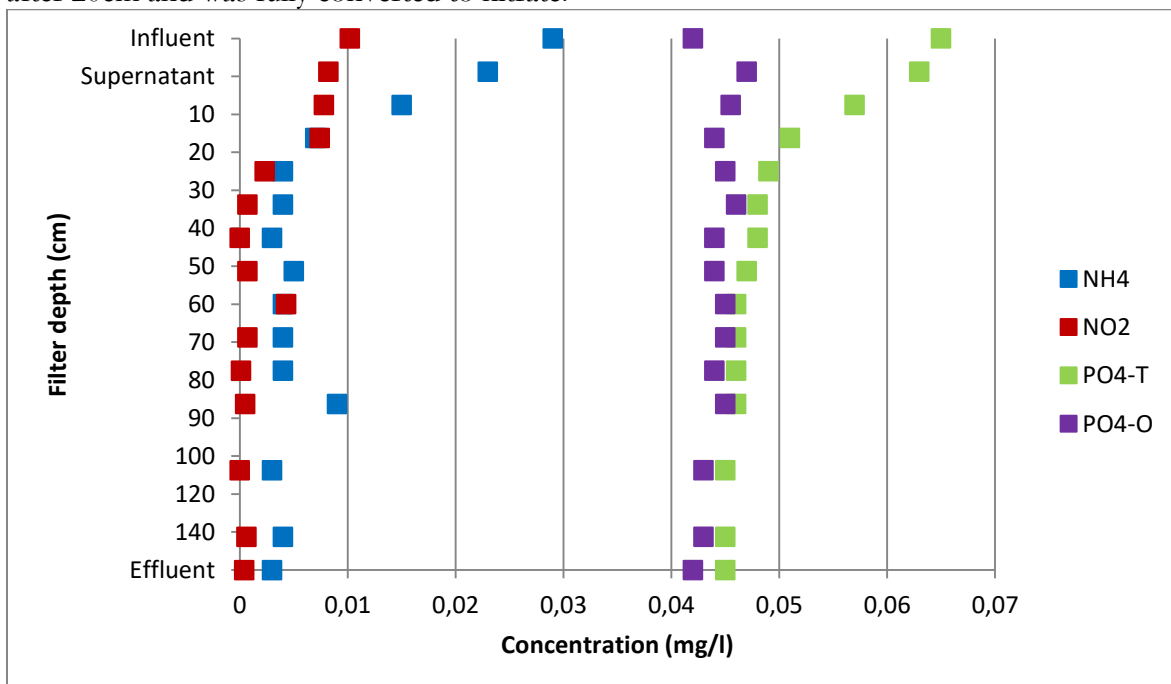


Figure 13: Nitrification, denitrification and phosphate behaviour over the height of the filter bed of RSF 8A in Katwijk

Experiments executed in the pilot showed similar results for  $\text{NO}_2$ ,  $\text{NH}_4$  and Mn concentrations in the effluent of the filter as is shown in Table 10(Appendice A).

### 4.3 Optimization of the chemical doses

In Table 5 the results of the optimization of the dosing are shown. The first setting was based on the results of the jar tests performed by KWR (Ahmad, 2017).

Table 5: Dosing optimization results

Setting	NaMnO <sub>4</sub> dosage (mg/l)	Fe(III) dosage (mg/l)	As (III) in supernatant (µg/l)	Residual As (µg/l)
reference	0	0	0.833	2.7
1	0.5	1.0	0.125	0.8
2	0.25	1.0	0.12	1.2
3	0	1.0	0.252	1.3
4	0	0.7	Not measured	1.4
5	0.4	0	Not measured	3.4

As shown in Table 5 when reducing the amount of MnO<sub>4</sub> dosed the residual As concentration in the effluent of the pilot filter increased. Furthermore it can be seen that the As(III) concentration in the supernatant increased. However, based on the As(III) in the supernatant of setting 2 it can be concluded that the dosing of 0.5 mg NaMnO<sub>4</sub> /l (for the purpose of As(III) oxidation) may have been excessive as no difference in As(III) concentration was observed while dosing 0.25 mg NaMnO<sub>4</sub> /l compared to 0.5 mg NaMnO<sub>4</sub> /l. This was also visible in jar tests performed by KWR (Ahmad et al., 2017b). MnO<sub>4</sub> doesn't play a big role in the removal of As(V) itself. The difference between the residual As in setting 1 and 2 in the effluent can't be explained because of the reduced dosing of MnO<sub>4</sub> because the removal of As by adsorption on MnO<sub>x</sub> is very small compared to the adsorption onto Fe(OH)<sub>3</sub> (Sorlini and Gialdini, 2010).

When comparing the residual As concentration for setting 2 and 3, the difference between dosing 0.25 MnO<sub>4</sub> or not was minor (0.1µg/L), raising the question whether dosing of MnO<sub>4</sub> is an effective additive in dune filtrate where only a portion of the arsenic was found to be As(III). Having said this, the target residual As concentration of <1 µg/l was only achieved with the setting Fe(III) dosage of 1 mg/l and MnO<sub>4</sub> dosage of 0.5 mg/L; all lower dosages of either Fe(III) or MnO<sub>4</sub> resulted in As>1 µg/L. Therefore, AOCF setting of 0.5 mg/L MnO<sub>4</sub> in combination with 1 mg/L Fe(III) was chosen by Dunea for further research.

#### 4.4 Effect of filter media and filtration velocity on arsenic removal

Samples used for analysis for As were taken from the influent, supernatant and effluent. Occasionally some samples were taken over the height over the filter bed to analyze the As concentration over the bed height and to see where the As removal takes place.

Table 6 and Table 7 show the average dissolved As concentration in the influent and the effluent and the total As removal efficiency as function of filtration media and velocity.

**Table 6: Average arsenic removal efficiency at various filtration velocities in the pumice filter (n =6)**

Filtration velocity	Dissolved As influent ( $\mu\text{g/l}$ )	Dissolved As effluent ( $\mu\text{g/l}$ )	Removal %
4 m/h	2.1 $\pm$ 0.17	0.67 $\pm$ 0.25	68%
6 m/h	2.3 $\pm$ 0.05	0.84 $\pm$ 0.49	64%
10 m/h	2.5 $\pm$ 0.18	0.71 $\pm$ 0.27	72%

**Table 7: Average arsenic removal efficiency at various filtration velocities in the anthracite filter (n=6)**

Filtration velocity	Dissolved As influent ( $\mu\text{g/l}$ )	Dissolved As effluent ( $\mu\text{g/l}$ )	Removal %
4 m/h	2.1 $\pm$ 0.17	0.77 $\pm$ 0.12	63%
6 m/h	2.4 $\pm$ 0.13	0.98 $\pm$ 0.40	59%
10 m/h	2.5 $\pm$ 0.18	0.54 $\pm$ 0.16	78%

**Table 8: Estimated contact times in each layer, based on porosity of 0.4 of sand and 0.5 of anthracite and pumice.**

Filtration velocity	Contact time with anthracite layer (min)	Contact time with sand layer (min)	Contact time with whole filter (min)
4 m/h	3.75	6	9.75
6 m/h	2.5	4	6.5
10 m/h	1.5	2.5	3.9

As can be seen in Table 6 and Table 7 there was no clear indication of an increase or decrease in removal efficiency. It appears - based on a small sample size - that the removal efficiency was not tied to the contact time (in the top layer of the filter) (Table 8) between the iron hydroxide flocs (formed by dosing  $\text{FeCl}_3$ ) and the As(V) in the water. This means that the contact time between the  $\text{MnO}_4$  and As(III) and between Fe(III) and As(V) was sufficient even at a filtration velocity of 10 m/h. For the oxidation of As(III) by  $\text{MnO}_4$  this was expected as this oxidation reaction occurred rapidly (Sorlini and Gialdini, 2010), but based on these results it is apparent that also As(V) sorption (onto Fe flocs) was not kinetically limited during filtration.

Based on the results achieved in Table 6 and Table 7 there is no clear difference in residual As concentration between the use of anthracite or pumice as the top layer. Even though the lowest average residual As concentration was observed in the anthracite filter at 10 m/h (0.54  $\mu\text{g/L}$   $\pm$  0.16), the pumice filter produced water containing slightly lower As at 4, 6 m/h. The pumice used is coarser than anthracite and thus allows iron flocs to penetrate deeper into the filter, this caused a small visible difference in As removal. In Figure 14 and Figure 15 the dissolved As is shown at various locations in the filterbed for both anthracite and pumice filter. It can be seen that in the supernatant of both the anthracite- and pumice-filter most of the As was already bound to the available iron flocs. After the initial removal in the top layer a small removal was seen in the next 50cm after which the As concentration stabilized.

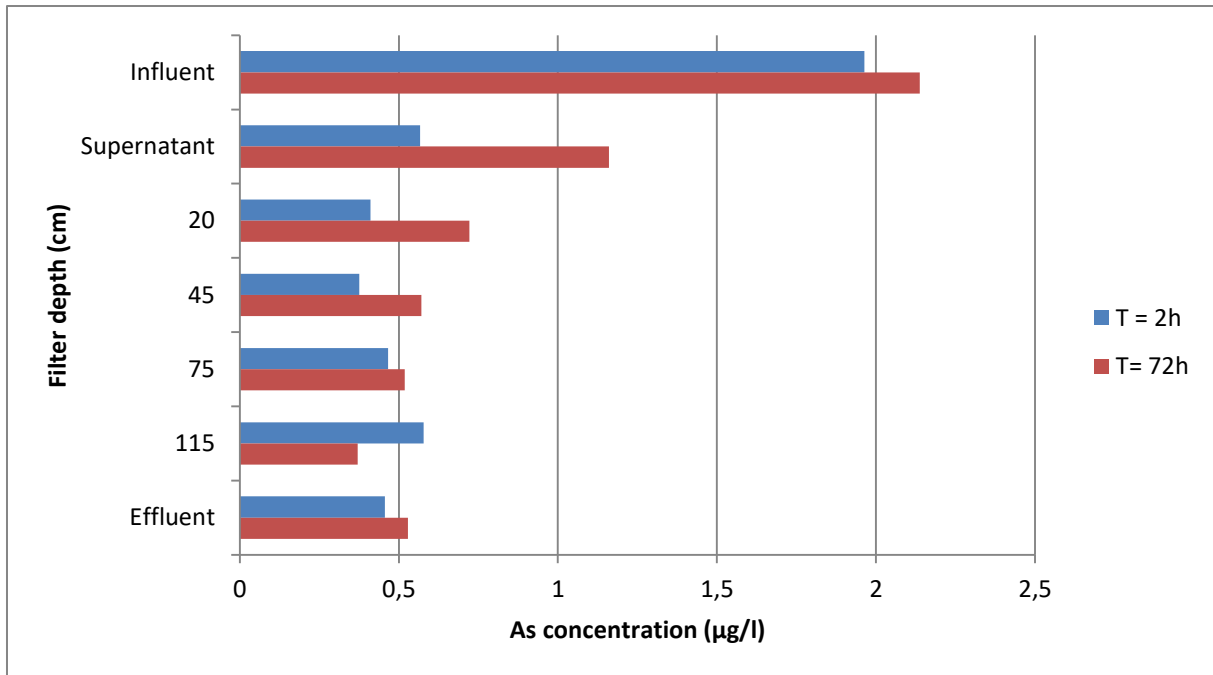


Figure 14: Behaviour of dissolved As in the pumice filter over the runtime, dosing 0.5 mg NaMnO<sub>4</sub> /l and 1.0 mg Fe(III)/l at filtration velocity of 4m/h

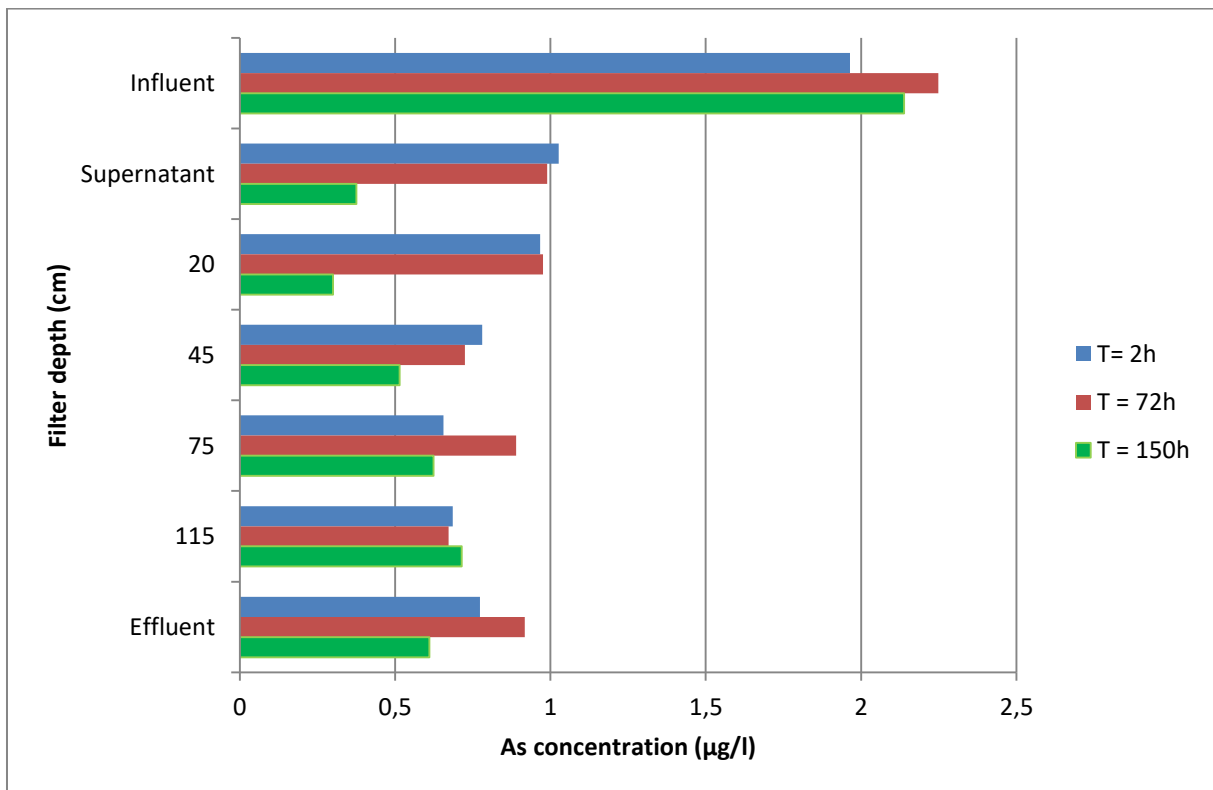


Figure 15: Behaviour of dissolved As in the anthracite filter over the runtime, dosing 0.5 mg NaMnO<sub>4</sub> /l and 1.0 mg Fe(III)/l at filtration velocity of 4m/h

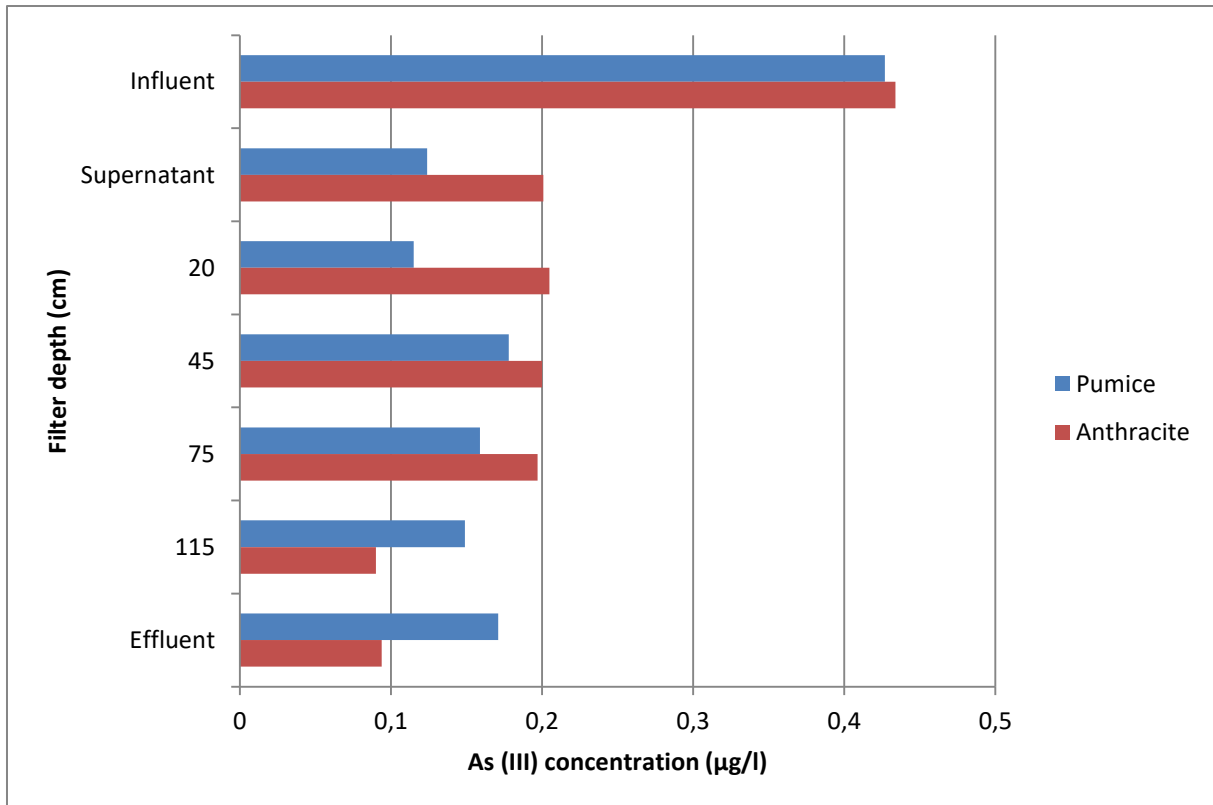


Figure 16: As(III) concentration over the filter height at 6 m/h

Figure 16 shows the As(III) concentration over the height of the pilot filters. There is no clear difference in As(III) concentration. In the anthracite filter some additional As(III) removal was seen in the bottom of the filter. However, due to the low concentrations that are observed analysis uncertainties may have played a huge role in these results. It can however be seen that the oxidation of As(III) was never fully complete even while dosing an stoichiometric overdose of  $\text{NaMnO}_4$ .

## 4.5 Pressure losses

### 4.5.1 Pressure losses caused by changing filtration velocity

To make a comparison regarding the pressure losses all measurements have been normalized to 4 m/h. This means that during the measurements while applying a filtration velocity of 6 or 10 m/h the filtration velocity was lowered to 4 m/h to do the measurements. This was required due to the influence of velocity on the pressure loss as was seen in the Carman-Kozeny equation. To ensure the columns were in equilibrium the velocities were set back for 45 minutes before doing the measurement. After the measurement the flow was increased again to the setting it was on prior to doing the measurement the filtration velocity was then increased again to 6 or 10 m/h.

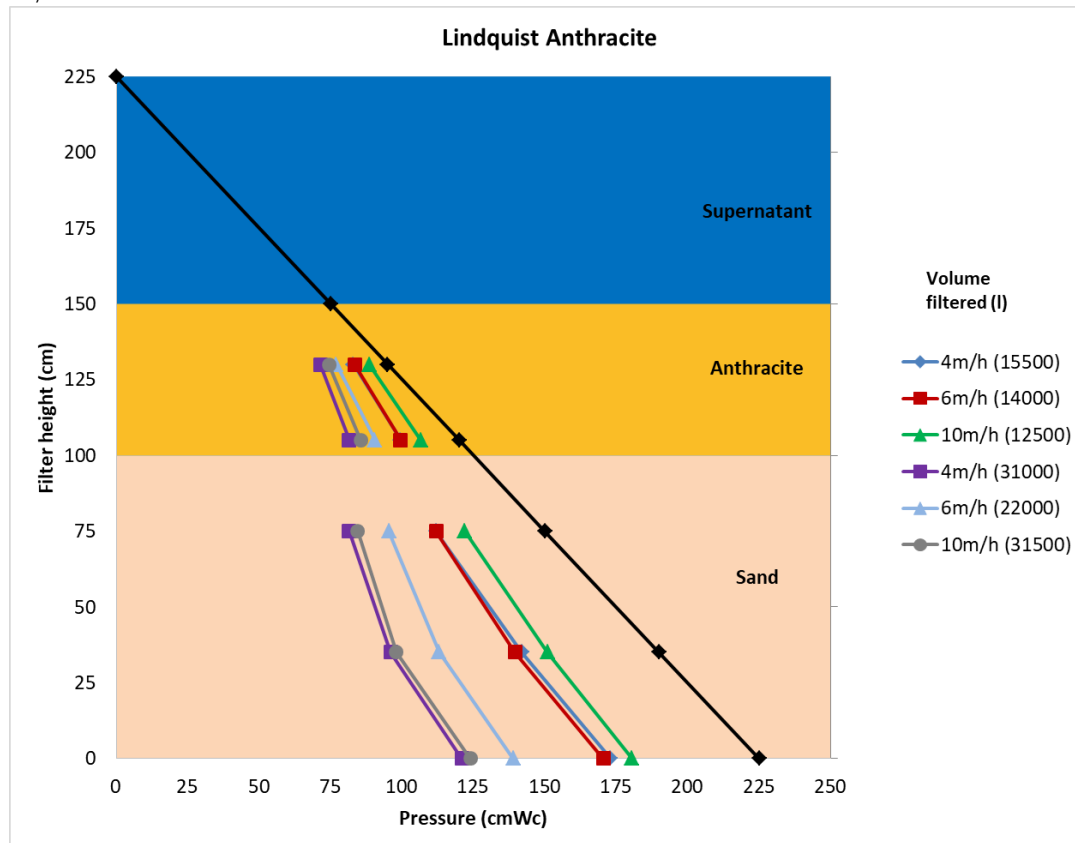


Figure 17: Normalized Lindquist diagram for the anthracite filter at 4,6,10 m/h while dosing 0.5mg NaMnO<sub>4</sub>/l and 1.0 mg Fe(III)/l

As is shown in Figure 17 the resistance in the anthracite filters remained relatively the same, even at higher filtration velocities. After treating 31000l both the experiment at 4m/h and at 10 m/h showed a pressure loss of about 1m. At higher filtration velocities it can be seen that the resistance build up in the top layer of the filter was smaller than at lower filtration velocities. However due to the higher amount of clogging in the top layer at lower filtration velocities it was expected that the sand layer was significantly less clogged and would therefore be lower in pressure loss. However as shown in Figure 17 this is not the case for the anthracite filter.

The resistance was built up relatively evenly between the top layer (anthracite) and the bottom layer (sand). There were no big jumps due to the clogging of a specific layer.

At higher filtration velocity it can be seen that even less resistance was built-up in the pumice layer. Our hypothesis is that this was possibly caused by the shear stress on the particles induced by higher flow velocities. Due to the higher flow velocities it is possible that the iron flocs broke down into smaller particles. These smaller particles could possibly more easily pass the pumice

layer compared to the bigger particles. The pumice layer therefore stored fewer particles at higher filtration velocities than at lower filtration velocities.

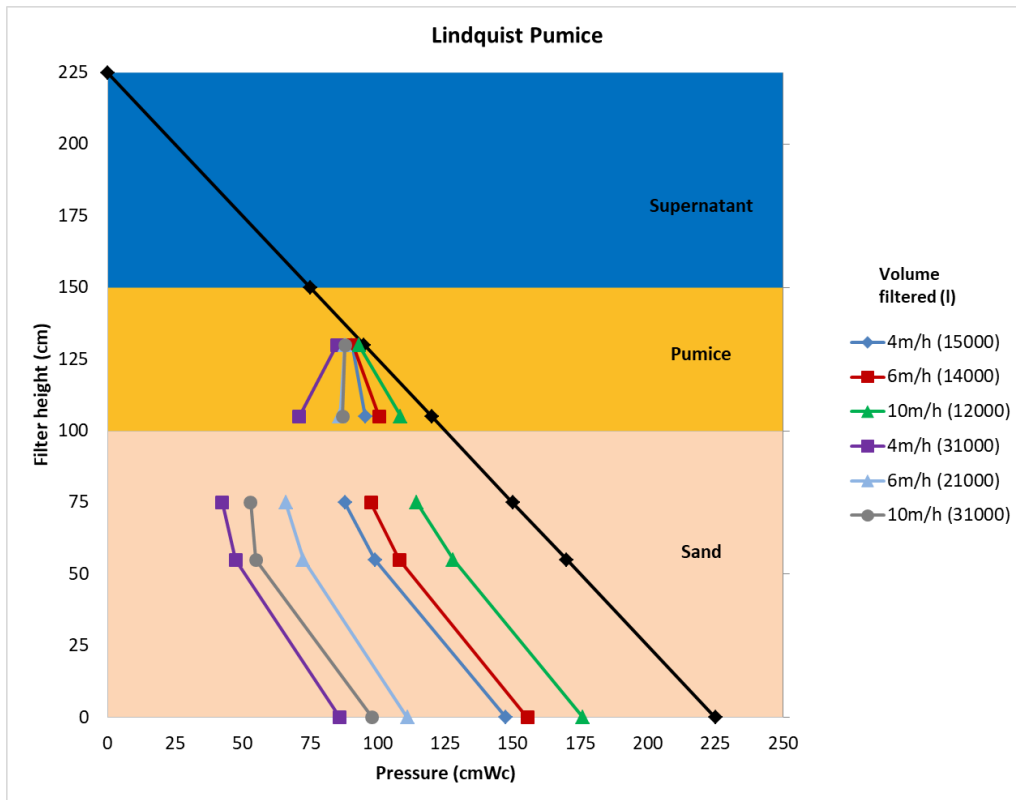


Figure 18: Normalized Lindquist diagram for the pumice filter at 4,6,10 m/h while dosing 0.5mg NaMnO<sub>4</sub> /l and 1.0 mg Fe(III) /l

#### 4.5.2 Pressure losses as function of filter media

In Figure 18 the Lindquist diagrams of the pumice filter are shown. The differences between the anthracite (Figure 17) and the pumice filter (Figure 18) were considerable. In the pumice filter at the start of the runtime we barely saw any pressure loss and thus no clogging. This may have occurred due to the larger particle size of the used pumice (2.5 – 3.5mm) compared to the used anthracite (1.6 – 2.5mm). This caused more small particles to pass through the top layer. This was also observed as a higher solids load on the sand layer. The pressure loss at the top of the sand layer was much bigger in the pumice filter compared to the sand in the anthracite filter (Figure 19). In the pumice filter, at a filtration velocity of 4m/h, after 31000l a pressure drop of 25cm was seen at the top layer of the sand. This pressure loss was very big compared to the <5cm pressure loss in the top of the sand layer in the anthracite filter. Due to the considerable clogging of the sand layer in the pumice filter the pressure loss over the whole filter increased significantly. It was however expected that the pumice filter would facilitate lower pressure losses due to the coarser grain sizes and particle storing volume available in the pumice.

This particle storing volume was not used because of the coarse particle size of the top layer media. This may have caused that most particles passed through the pumice layer (causing no clogging in the pumice and thus a very low pressure loss) and caused the particles to be removed by the top layer of the sand instead. The sand layer in the pumice filter was thus loaded with more particles that were filtered by the sand. Because of the pass-through through the top layer it can also be assumed that the average size of the particles that are filtered by the sand was also bigger than during the filtration in the anthracite filter. This caused the top layer of the sand to clog and cause high pressure losses. The anthracite filter had a more even distribution of particles

and therefore only a small pressure loss occurred in the sand layer. At the end of the experiments (after treating the same amount of water) the anthracite filter had lower total pressure loss (73 cmWc) than the pumice filter (95 cmWc). In Table 9 all pressure loss results are shown for various volumes treated. Anthracite consistently showed lower pressure losses than the pumice filter. The difference between the pumice and anthracite filter increased when the filtration velocity increased.

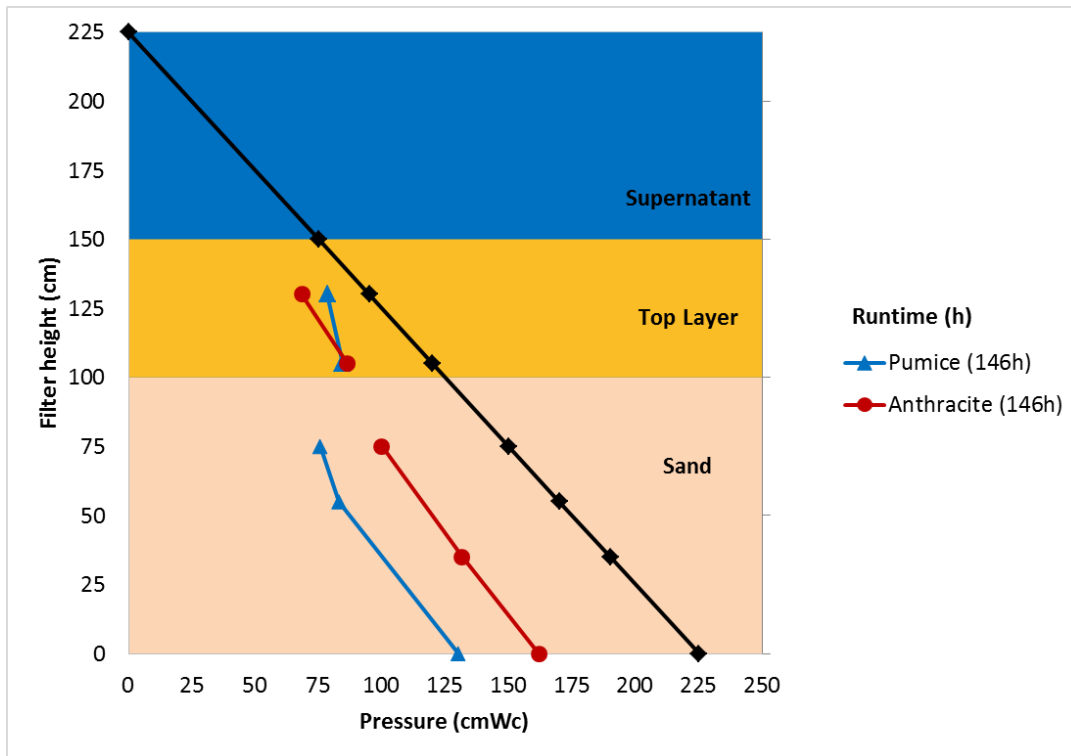


Figure 19: Comparison of pressure loss between the pumice and anthracite filter

Table 9: Pressure loss results of both pilot filters at 1.0 mg Fe(III) /l and 0.5 mg NaMnO<sub>4</sub> /l

Filtration velocity	Filter	Pressure loss at 14000l	Pressure loss at 32000l
4 m/h	Anthracite	25.5	83.5 ( $\pm 10.5$ )
	Pumice	27.5 ( $\pm 3$ )	110 ( $\pm 11$ )
6 m/h	Anthracite	33.5	-
	Pumice	37	-
10 m/h	Anthracite	44.5	101
	Pumice	49	132 ( $\pm 5$ )

## 4.6 Runtime

Currently the full scale rapid sand filters at WTP Katwijk are backwashed based on a specific runtime of 7 days. Due to the added dosing of Fe(III) the runtime of the filters was expected to decrease due to either resistance build-up in the filters or due to breakthrough occurring earlier (Dunea, 2011).

In Figure 20 and Figure 21 the relation between the filtration velocity and breakthrough is shown. For both the anthracite and pumice filters the breakthrough time was determined and expressed as treated volume. As can be seen in Figure 20 and Figure 21 the volume that could be treated at higher filtration velocities decreased when the filtration velocity increased. This might have been caused by the lower efficiency of filtration at higher velocities and thus particles passing through quicker (van Dijk, 2010). The runtime corresponding with the volumes was 130, 68 and 22.4 hours for respectively a filtration velocity of 4, 6 and 10 m/h. At a filtration velocity of 4 m/h this meant a runtime of 130h and thus <6 days. This means that the condition for backwash may shift from pressure loss to breakthrough.

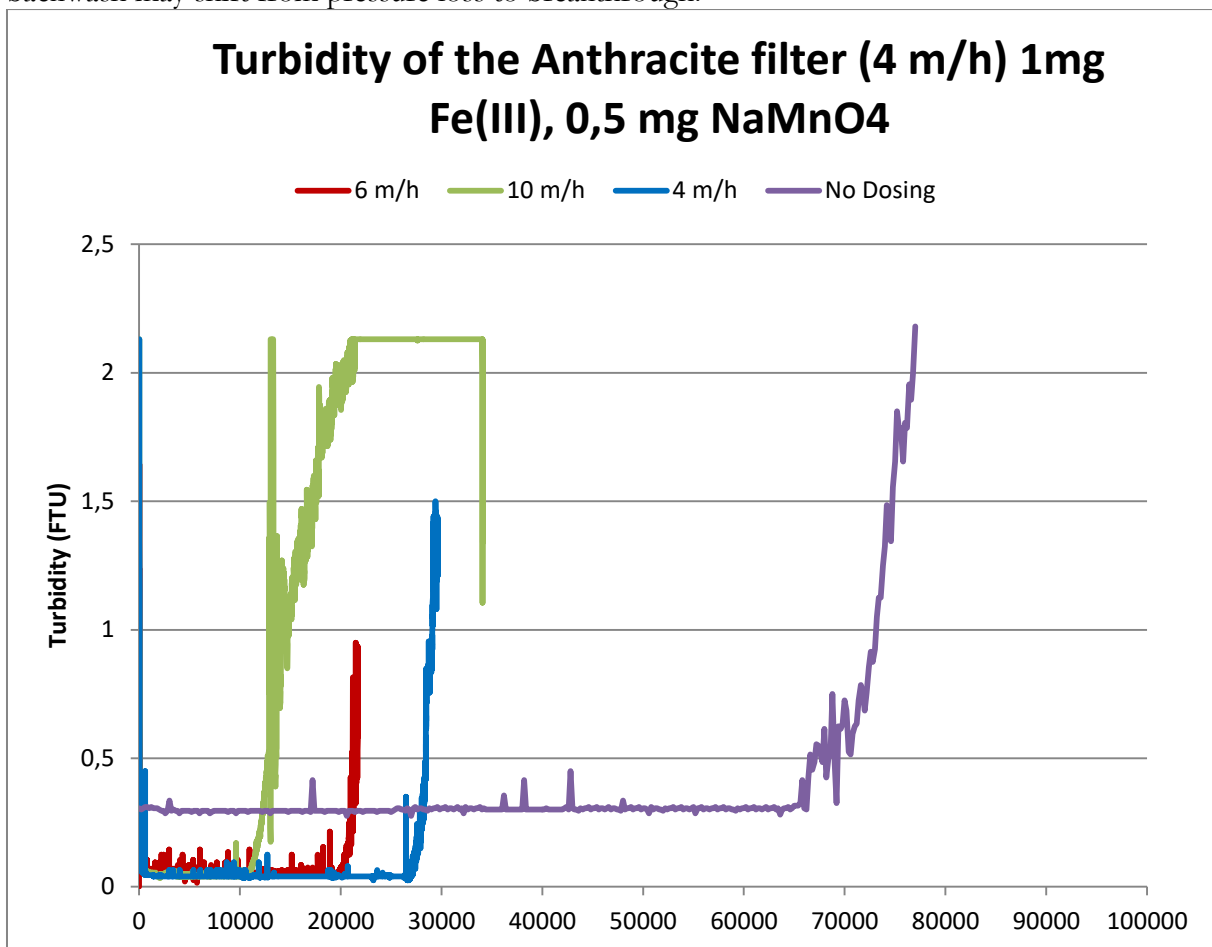


Figure 20: Breakthrough of the anthracite pilot filter with and without AOCF

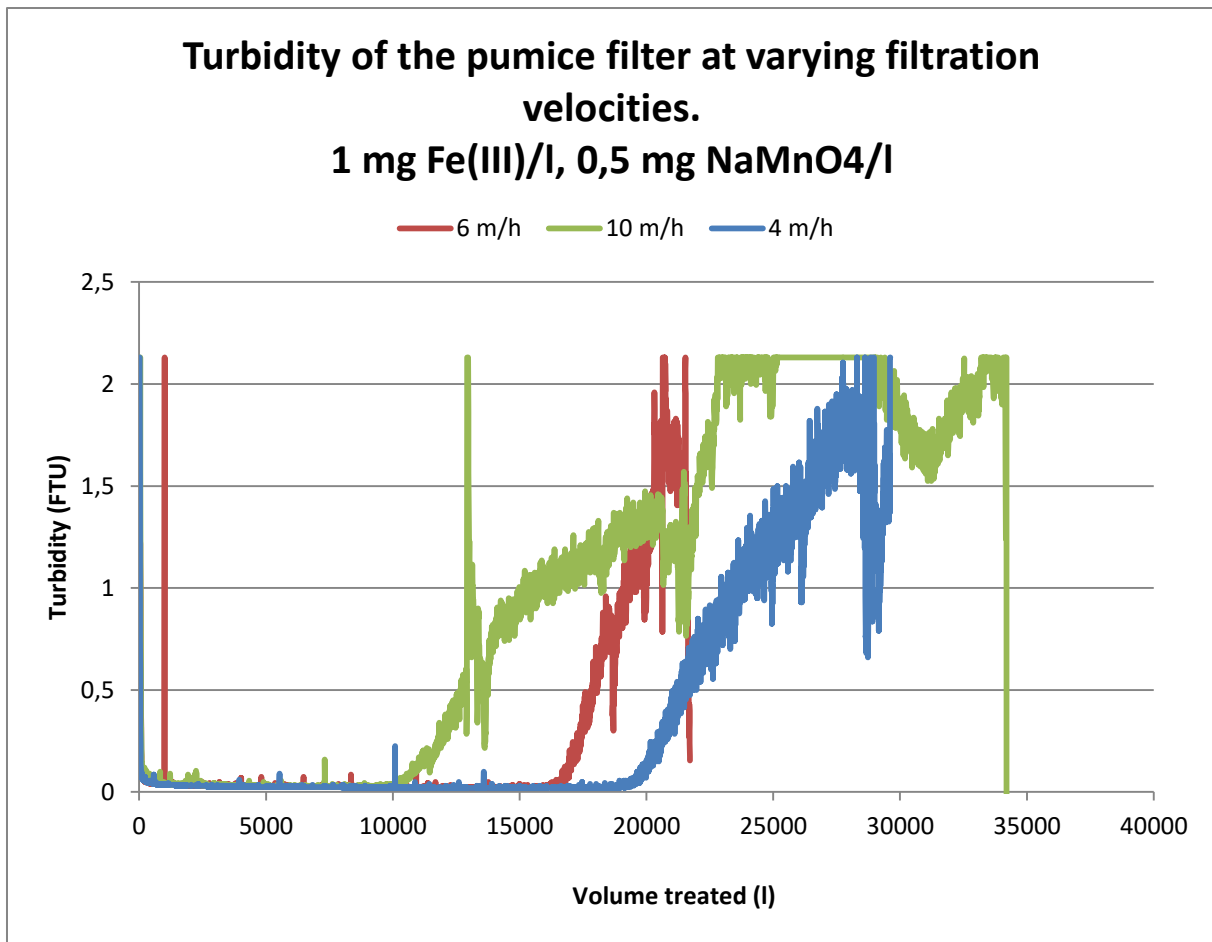


Figure 21: Turbidity of the pumice filter at varying filtration velocities

Figure 20 shows the comparison of the breakthrough of the filter while applying AOCF compared to the breakthrough without the application of AOCF. At 4 m/h the application of AOCF decreased the breakthrough time to about 5.5 days. The turbidity of the effluent however dropped from 0.3 FTU to about 0.03 FTU causing a lower load of particles on the final SSF step.

In Figure 22 the seemingly linear relation between filtration velocity and treated volume before breakthrough is shown (for these specific filters and this specific water). The relation is based on three points so it may be argued that data is limited.

Figure 22 also shows that anthracite was better suitable at lower filtration velocities while the difference between pumice and anthracite decreased when the filtration velocity increased. My hypothesis for this phenomena is that at higher filtration velocities more and more particles pass through the top layer. Therefore when the velocity increases some particles that would be removed by the anthracite top layer now pass through the anthracite. The bottom 1m of sand is identical and therefore when the velocity increases the breakthrough will occur at the same time.

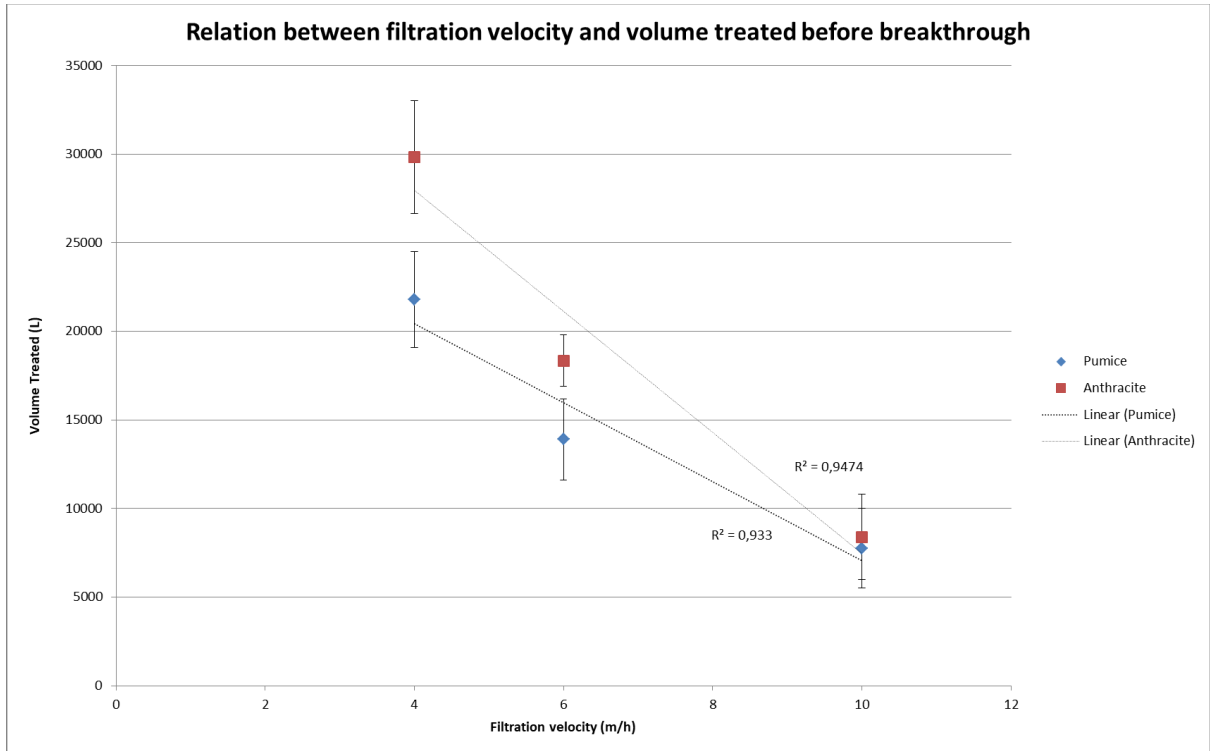


Figure 22: Volume treated before breakthrough vs filtration velocity

## 4.7 Backwash water settling tests

Figure 23a to Figure 25b show the results of the backwash water settling experiments that were performed. It was hypothesized that the sedimentation front velocity would increase due to the increase in particle size due to the presence of Fe(III).

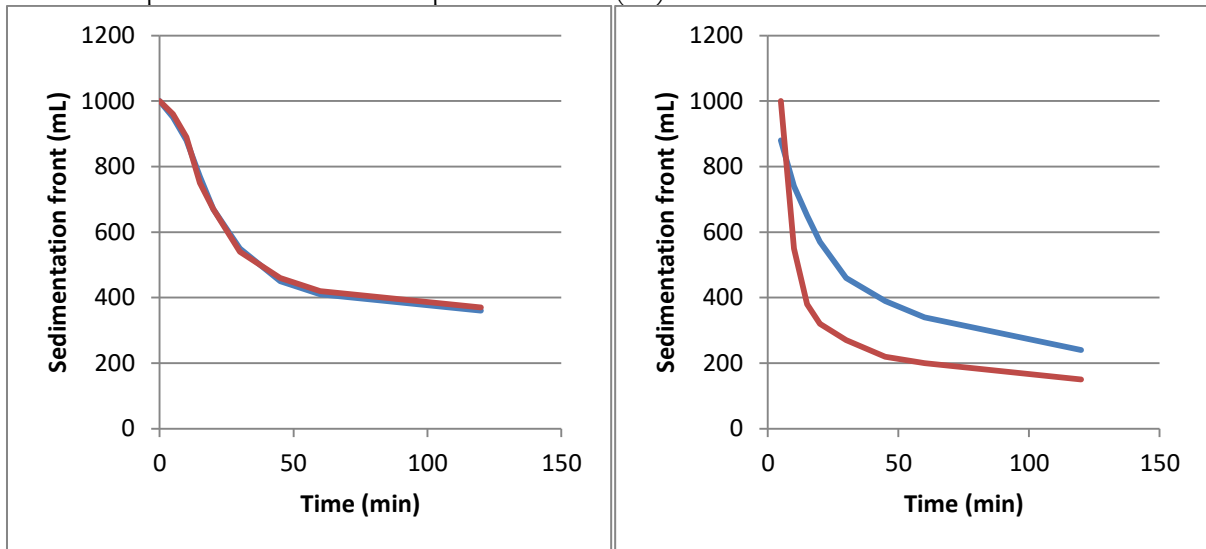


Figure 23a

Sedimentation front (ml) of backwash water at 4m/h. Left figure represents no dosages, right figure represents AOCF with dosages of 1.0 mg Fe(III)/l and 0.5 mg NaMnO<sub>4</sub>/l. Blue line represents anthracite pilot filter, red line represents pumice filter

Figure 23b

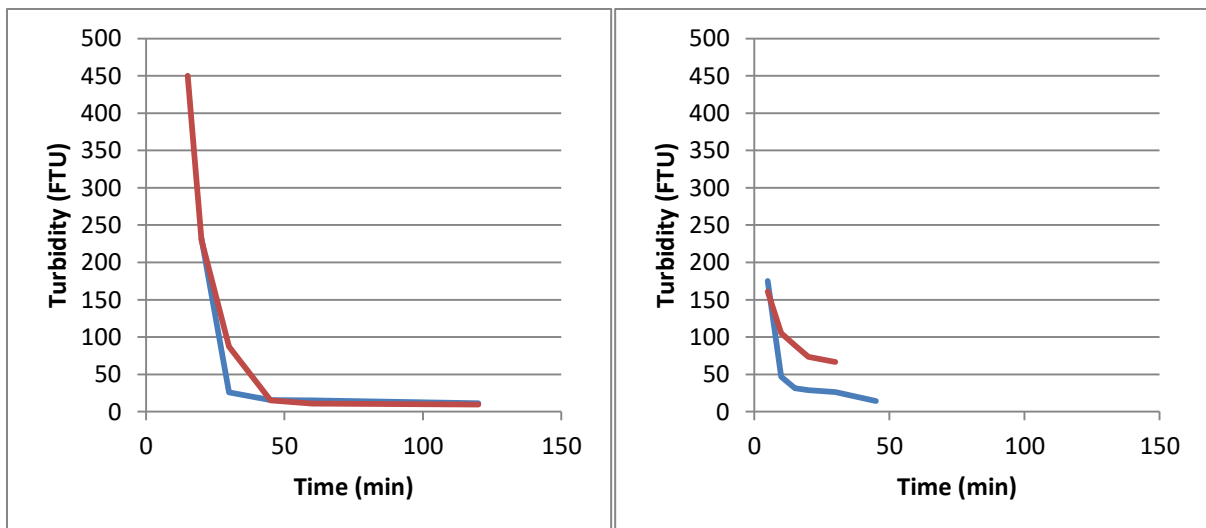


Figure 24a

Turbidity at 750ml of backwash water at 4m/h. Left figure represents no dosages, right figure represents AOCF with dosages of 1.0 mg Fe(III)/l and 0.5 mg NaMnO<sub>4</sub>/l. Blue line represents anthracite pilot filter, red line represents pumice filter

Figure 24b

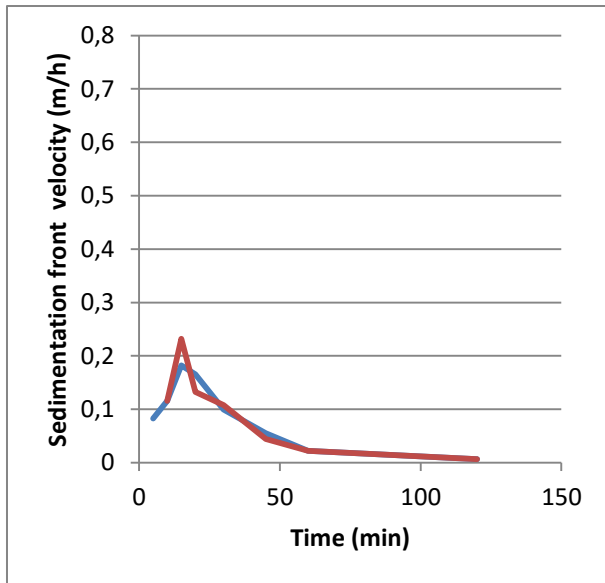


Figure 25a

Sedimentation front velocity (m/h) of backwash water at 4m/h. Left figure represents no dosages, right figure represents AOCF with dosages of 1.0 mg Fe(III)/l and 0.5 mg NaMnO<sub>4</sub> /l. Blue line represents anthracite pilot filter, red line represents pumice filter

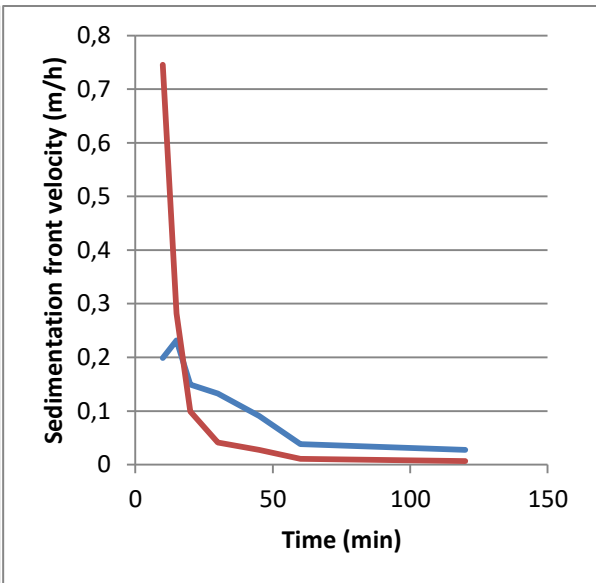


Figure 25b

Based on Figure 25a and Figure 25b it appears that after the addition of the AOCF process the sedimentation front moved quicker than in the initial situation. This means that the settling time of all the backwash water decreased.

Additionally, based on a secondary backwash experiment it can be seen that the sedimentation of the backwash water sludge originating from the AOCF pilot occurred much quicker than sedimentation of the sludge originating from the RSF in Katwijk without the application of AOCF. In Figure 26 and Figure 27 it can be seen that sedimentation occurred more rapidly in pilot backwash water.



Figure 26: Secondary backwash experiment T = 8 min, left contains backwash water from the pilot filter while applying AOCF, right jar is backwash water originating from a RSF in Katwijk



Figure 27: Secondary backwash experiment  $T = 26$  min, left contains backwash water from the pilot filter while applying AOCF, right jar is backwash water originating from a RSF in Katwijk

## 5. Conclusions and recommendations

### 5.1 Conclusions

From the results from all the experiments there are several conclusions that can be drawn considering the Fe(III) – MnO<sub>4</sub> dosing.

- In Katwijk a residual concentration of <1 µg/l can be reached by dosing a combination of Fe(III) and MnO<sub>4</sub>. The dosing that consistently reaches a residual As concentration of <1 µg/l is 1.0 mg Fe(III)/l and 0.5 mg NaMnO<sub>4</sub> /l.
- Arsenic removal by the use of Fe(III) – MnO<sub>4</sub> dosing does not seem to be affected by filtration velocity. At higher filtration velocity the As removal still takes place and the efficiency does not seem to go down. This is caused by the fact that most of the As removal takes place in the upper 20 cm of the layer of the filter.
- In this study the anthracite used (1.6 - 2.5mm) was better suited as the top layer for treating the influent of Katwijk. The Pumice used in the experiments (currently used in Scheveningen (2.5-3.5mm)) is too coarse and causes a higher load on the sand layer under the pumice. This causes a less efficient distribution of particles stored in the whole bed. Due to the faster clogging of the sand the pressure loss in the filters with this specific pumice as top layer was greater than when using the anthracite regarded in this study as a top layer.
- The runtime of the pilot filters in Katwijk decreased significantly. Without the dosing of any chemical the runtime of the filters was about 16 days. Including the dosing (1 mg Fe(III) and 0.5 mg NaMnO<sub>4</sub>) however the runtime (at a filtration velocity of 4 m/h) decreased to about 6 days when 0.5 mg NaMnO<sub>4</sub> /l and 1.0 mg Fe(III)/l were dosed to remove As. This runtime is based on the breakthrough of the filter and is not determined anymore by the pressure loss. Breakthrough has become the limiting factor, whereas in the current full-scale filters – without AOCF - the pressure loss is determining. However, in the RSFs in Katwijk the runtime – based on pressure loss – is already 7 days without the application of AOCF. When applying AOCF on filters with mudballs the runtime will most likely decrease further.
- Iron, Manganese, Ammonia and nitrite levels in the effluent do not increase during normal process. All the processes remained stable during the 9 months the pilot has functioned. Additionally Filtration performance is enhanced when 1.0 mg Fe(III) /l and 0.5 mg NaMnO<sub>4</sub> /l are dosed. The turbidity of the effluent drops from 0.2-0.3 FTU to about 0.030 FTU in both the anthracite and the pumice filter. This drop in turbidity is very important for the SSF step afterwards as the filters will be clogged less often than the current situation. Cleaning of the SSF is an intensive and costly process and therefore a reduction in clogging is very beneficial.
- Based on preliminary settling experiments it appears that the settling velocity of the backwash water increases. However more research is required on this topic to draw definitive conclusions.

## 5.2 Recommendation for the application at Katwijk

### 5.2.1 Pilot results

The presented research has provided evidence that AOCF, consisting of dosing 0.5 mg/L  $\text{KMnO}_4$  and 1 mg/L  $\text{Fe(III)}$  is capable of consistently removing As to concentrations  $<1\text{ug/L}$  at Katwijk. This technology is therefore a ready to implement solution for Dunea to directly reach the new company target of  $1\text{ug/L}$ . Nevertheless, it was also found in this research that runtimes are seriously reduced when applying AOCF, leading to potential problems in the backwash water treatment facilities of the plant. Therefore it is also recommend to further investigate if the current dosing of  $\text{KMnO}_4\text{-Fe(III)}$  could be replaced, or lowered in concentration. Dune effluent consists predominantly of As(V) and may thus potentially be treated without an oxidant. However, this would require additional research to investigate improving As(V) sorption onto precipitating HFO flocs.

### 5.2.2 Differences between the pilot filter and the filters in Katwijk

From a water quality perspective, the pilot filter has shown to provide a solid simulation of the full-scale RSF's at Katwijk. However, when reviewing the pressure losses – and thus clogging - over time, the pilot filter (when AOCF is not applied) behaved very different from the full scale RSF's (Figure 28). This can potentially be explained by the mudballs that have recently appeared on the top layer of the RSF. Mudballs are balls of mud formed by small particles of organic material. When formed, these mudballs are not sufficiently removed by the current RSF backwash program. This causes an agglomeration of mudballs on the top of the filter and therefore clogging this layer. The clogging of the top layer causes high pressure losses and therefore a shorter runtime. Currently the RSF's are backwashed after approximately 7 days. During this runtime the pressure loss over the filter is increased from about 0.13m (clean bed resistance) to approximately 1.3m. In 2002 it was reported that the RSF's in Katwijk had an average runtime of approximately 10 days (Dunea, 2002).

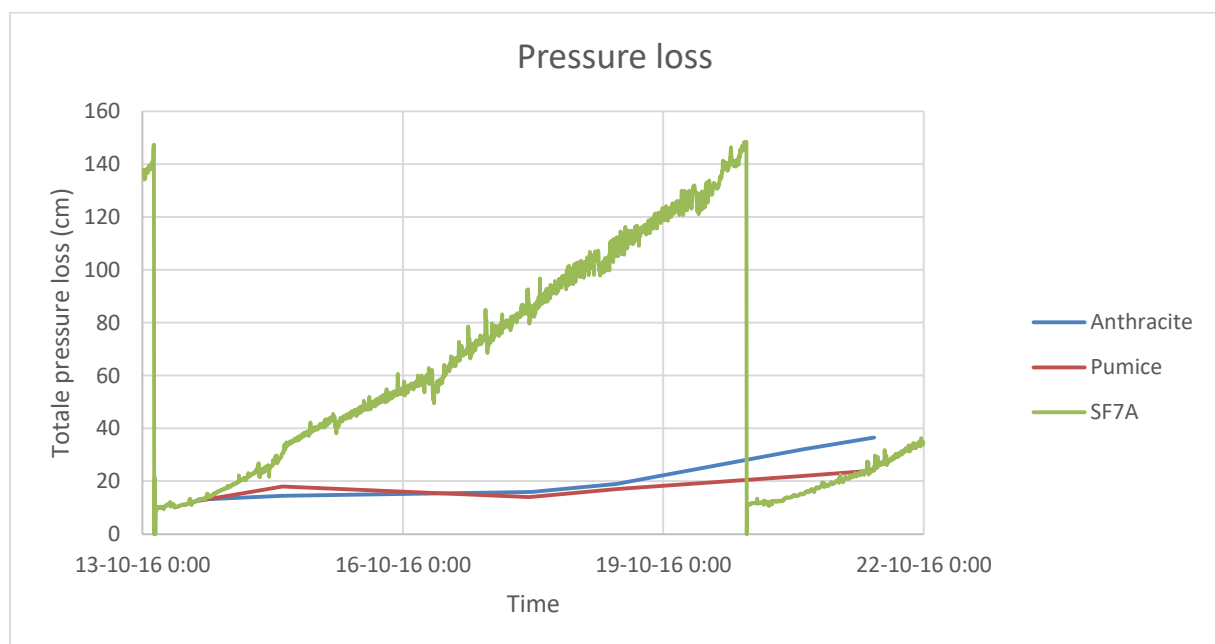


Figure 28: Pressure loss over the whole filter over time without the application of AOCF. SF7A is one of the 20 RSF's at DWTP Katwijk.

In the pilot it was found that the runtime decreases (when AOCF is applied on the current filters with mudballs in Katwijk) by about 50% compared to the initial condition. In the pilot filter this decreases to about 6 days, the RSFs in Katwijk (with mudballs) however, start at 7 days. When reducing the 7 days by 50% the runtime will decrease to about 3.5 days. This runtime is currently not feasible with the current backwash water system. Therefore the backwash water treatment may have to be adjusted if AOCF is applied at the current mudballs polluted filter.

However if additional research to settling properties show the improved settling properties it may be possible to reduce the settling time set for a batch of backwash water. If this time can be reduced; more batches of backwash water can be treated on a daily basis and thus the backwash water treatment capacity will increase. However this increase alone can most likely not deal with double the current backwash water.

It is therefore recommended that the mudball problem that currently exists is solved before any full scale application experiments are executed. When this problem is fixed and the filters are clean and fully functional the AOCF can be tested in a full scale experiment. It is recommended to start with dosages found in this thesis (1.0 mg/l  $\text{FeCl}_3$  and 0.5  $\text{NaMnO}_4$ ). The dosages can then be further optimized in full scale experiments. Minimizing the use of  $\text{FeCl}_3$  has the highest priority as this influences the runtimes of the RSFs tremendously. To optimize the  $\text{MnO}_4$  dose, As(III) has to be measured preferably just above the filter bed. Based on the amount of As(III) available the  $\text{MnO}_4$  dosage can be decreased slightly until the As(III) start increasing.

### 5.2.3 Additional research

Most of the research done has been focused on the effect of  $\text{MnO}_4$  on As. At Dunea however PAC is available in the water. The PAC may have a negative effect on the  $\text{MnO}_4$  as it may help the  $\text{MnO}_4$  reduce to  $\text{MnO}_x$  (Zhang et al., 1997). A proposal for jar test experiments to investigate this is shown in Appendix D.

Furthermore the usage of the PAC by  $\text{MnO}_4$  will influence the availability of PAC for the original goal. This may lead to insufficient PAC available for the treatment process itself. More research is may be necessary to the effectiveness of the PAC after dosing  $\text{FeCl}_3$  and  $\text{NaMnO}_4$  in the water before RSF.

More research to the settling properties of the new backwash water may be required. Based on the small experiments it appears that the settling velocity increases, but Brabant Water has reported changes in the dewatering properties of the sludge. These changes are important for the whole backwash water treatment and should be considered.

## References

- AHMAD, A. 2014. Evaluation and optimization of advanced oxidation coagulation filtration (AOCF) to produce drinking water with less than 1 µg/l of arsenic.
- AHMAD, A. 2017. DPWE: Towards achieving <1 µg/L arsenid at Katwijk, Ouddorp and Leiduin.
- AHMAD, A., VAN DE WETERING, S., GROENENDIJK, M. & BHATTACHARYA, P. 2014. Advanced Oxidation-Coagulation-Filtration (AOCF) - An innovative treatment technology for targeting drinking water with <1 µg/l of arsenic. 817-819.
- AHMAD, A., VAN DIJK, T., VAN DE WETERING, S., GROENENDIJK, M. & BHATTACHARYA, P. 2017b. Best Practice Guide on the Control of Arsenic in Drinking water. IWA.
- BARRINGER, J. L. & REILLY, P. A. 2013. Arsenic in groundwater: a summary of sources and the biogeochemical and hydrogeologic factors affecting arsenic occurrence and mobility. In: BRADLEY, P. (ed.) *Current Perspectives in Contaminant Hydrology and Water Resources Sustainability*. InTech.
- BORA, A., GOGOI, S., BARUAH, G. & DUTTA, R. 2016. Utilization of co-existing iron in arsenic removal from groundwater by oxidation-coagulation at optimized pH. *Journal of Environmental Chemical Engineering*, 4, 2683-2691.
- BORDOLOI, S., NATH, S. K., GOGOI, S. & DUTTA, R. K. 2013. Arsenic and iron removal from groundwater by oxidation-coagulation at optimized pH: Laboratory and field studies. *Journal of Hazardous Material*, 260, 618-626.
- CHEN, W., PARETTE, R., ZOU, J., CANNON, F. S. & DEMPSEY, B. A. 2007. Arsenic removal by iron-modified activated carbon. *Water Research*, 41, 1851-1858.
- CLIFFORD, D. A., USEPA & AWWA 2004. *Field speciation method for arsenic inorganic species*, AWWA Research Foundation.
- DE MOEL, P. J., VERBERK, J. Q. J. C. & VAN DIJK, J. C. 2006. *Drinking Water Principles and Practices*.
- DISSANAYAKE, C. B. & CHANDRAJITH, R. 1999. Medical geochemistry of tropical environments. *Earth-Science Reviews*, 219-258.
- DUNEA 2002. Inventarisatie en optimalisatie snelfilters Productie.
- DUNEA 2011. Ijzerdosering op snelfilters Katwijk. Dunea.
- DUNEA 2016. Preparation of the AOCF pilot installation for the purpose of arsenic removal in the RSFs of Dunea at treatment location Katwijk.
- EPA 2015. Water Treatment Pilot Plant Design Manual: Low Flow Conventional/Direct Filtration Water Treatment Plant for Drinking Water Treatment Studies. EPA.
- HOLM, T. R., KELLY, W. R., WILSON, S. D., ROADCAP, G. S., TALBOTT, J. L. & SCOTT, J., S 2006. Arsenic distribution and speciation in the Mahomet and Glasford Aquifers, Illinois.
- KAWAMURA, S. 1999. Design and operation of high-rate filters. *AWWA Journal*.
- KERSTEN, M. & VLASOVA, N. 2009. Arsenite adsorption on goethite at elevated temperatures. *Applied Geochemistry*, 24, 32-43.
- LI, N., FAN, M., LEEUWEN, J. V., SAHA, B., YANG, H. & HUANG, C. P. 2007. Oxidation of As(III) by potassium permanganate. *Journal of Environmental Sciences*, 19, 783-786.
- MANNING, B., FENDORF, S., BOSTICK, B. & SUAREZ, D. 2002. Arsenic(III) Oxidation and Arsenic(V) adsorption Reactions on Synthetic Birnessite. *Environmental Science & Technology*, 36, 976-981.
- MAU, R. E. 1992. *Particle Transport in Flow Through Porous Media: Advection, Longitudinal Dispersion And Filtration*. Doctor of Philosophy, California Institute of Technology.
- SEVIL, C. 2005. Arsenic removal from groundwater by Fe-Mn oxidational microfiltration.
- SIDDIQI, S. I. & CHAUDHRY, S. A. 2017. Iron oxide and its modified forms as an adsorbent for arsenic removal: A comprehensive recent advancement, In Process Safety and Environmental Protection. *Process Safety and Environmental Protection*, 111, 592-626.
- SMEDLEY, P. L. & KINNIBURGH, D. G. 2001. Chapter 1. Source and behaviour of arsenic in natural waters. *United Nations Synthesis Report on Arsenic in Drinking Water*.

- SORLINI, S. & GIALDINI, F. 2010. Conventional oxidation treatments for the removal of arsenic with chlorine dioxide, hypochlorite, potassium permanganate and monochloramine. *Water Research*, 2010, 5653-5659.
- TUDELFT. 2017. OCW: *Granular filtration* [Online]. Available: <https://ocw.tudelft.nl/wp-content/uploads/Granular-filtration-1.pdf> [Accessed 6-10-2017 2017].
- VAN DIJK, J. C. 2010. Granular Filtration - Drinking Water Treatment 1. TUD Open Courseware website.
- VAN HALEM, D., BAKKER, S. A., AMY, G. L. & VAN DIJK, J. C. 2009. Arsenic in drinking water: A worldwide water quality concern for water supply companies. *Drinking Water Engineering and Science*, 2, 29-34.
- WHO 2001. Arsenic and arsenic compounds. World Health Organization, International Programme on Chemical Safety.
- WHO 2011. Arsenic in drinking water: Background document for development of WHO guidelines for drinking water quality. WHO.
- ZHANG, K., LI, C., HE, J. & LIU, R. 1997. Adsorption of permanganate onto activated carbon particles. *Journal of West China University of Medical Sciences*.

## Appendice A: Water quality parameters pilot compared to RSFs Katwijk

Table 10: Ammonium, nitrate, nitrite and Mn removal comparison between pilot and RSF Katwijk(Dunea, 2016)

Parameter	Unit	Value				
		26-9-2016			27-9-2016	13-9-2016
		Influent	Anthracite pilot installation	Pumice pilot installation	RSFs	
<b>Turbidity</b>	FTU	2.724	0.333	0.212	0.229	
<b>Ammonium</b>	mg/l NH <sub>4</sub>	0.0399	0.0052	0.0077		0.0386
<b>Nitrate</b>	mg/l NO <sub>3</sub>	1.4299	1.576	1.5804		1.9169
<b>Nitrite</b>	mg/l NO <sub>2</sub>	0.03612	0.007	0.007		0.00328
<b>Iron</b>	µg/l Fe	359	12.96	9.59	9.972	
<b>Manganese</b>	µg/l Mn	33.84	0.16	0.21	0.184	
<b>Arsenic</b>	µg/l As	4.06	2.82	3.19		

## Appendice B: Lindquist diagrams at 4, 6, 10 m/h

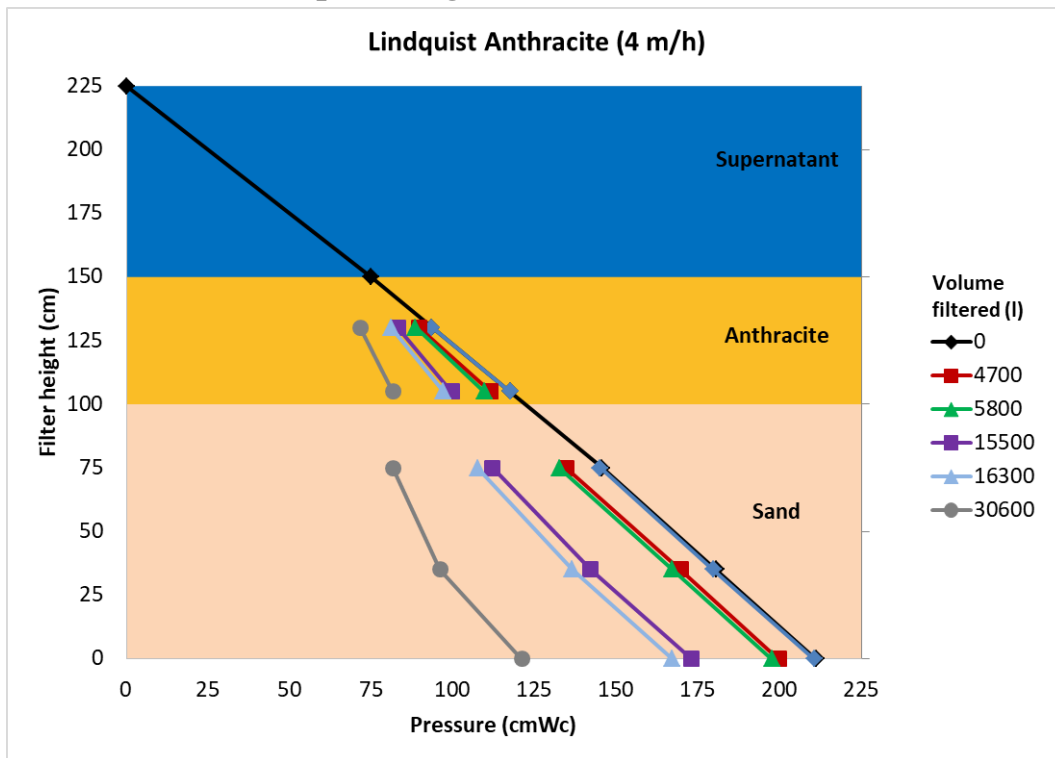


Figure 29: Lindquist diagram of the anthracite filter at a filtration velocity of 4 m/h

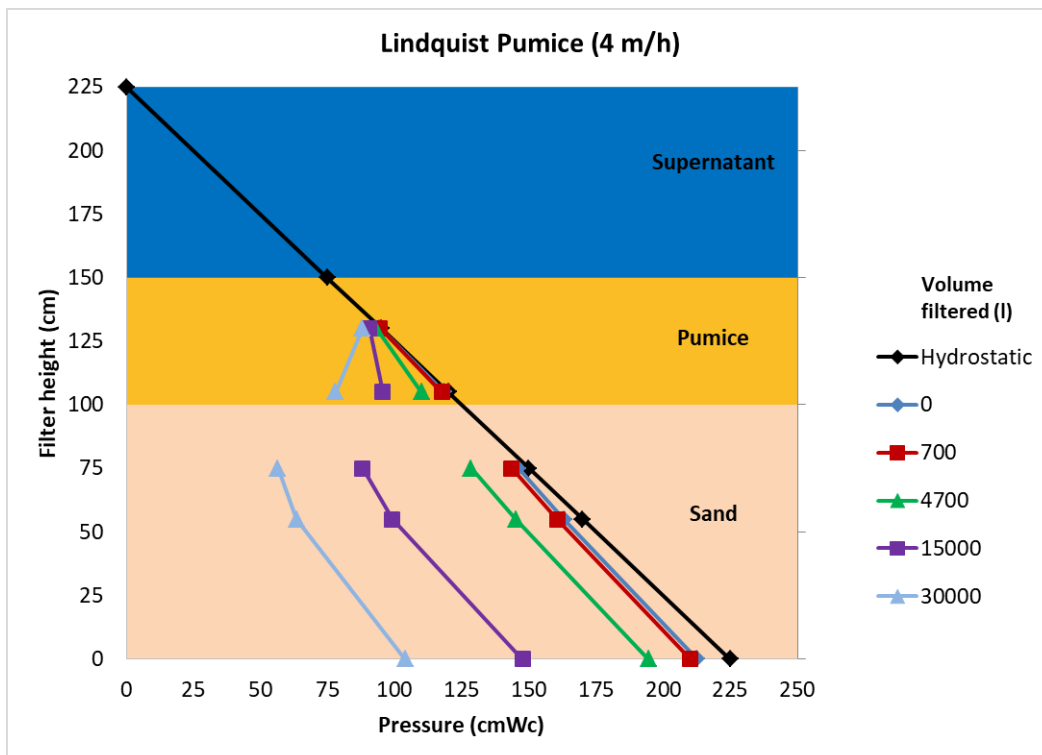


Figure 30: Lindquist diagram of the pumice filter at a filtration velocity of 4 m/h

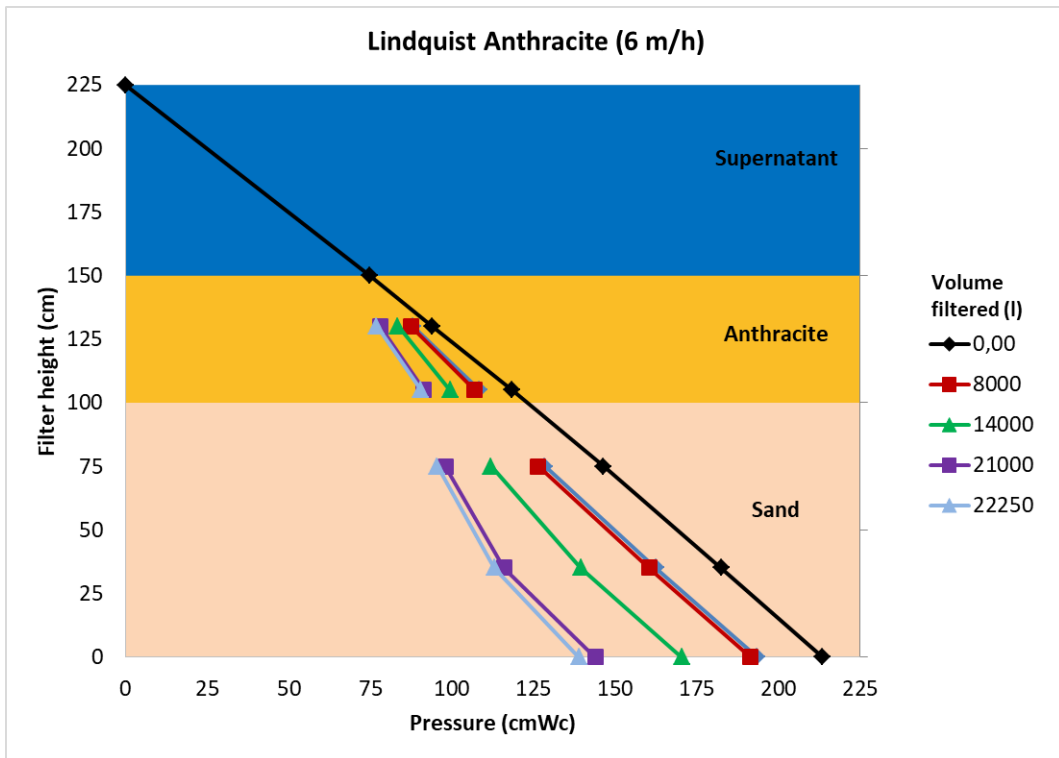


Figure 31: Lindquist diagram of the anthracite filter at a filtration velocity of 6 m/h

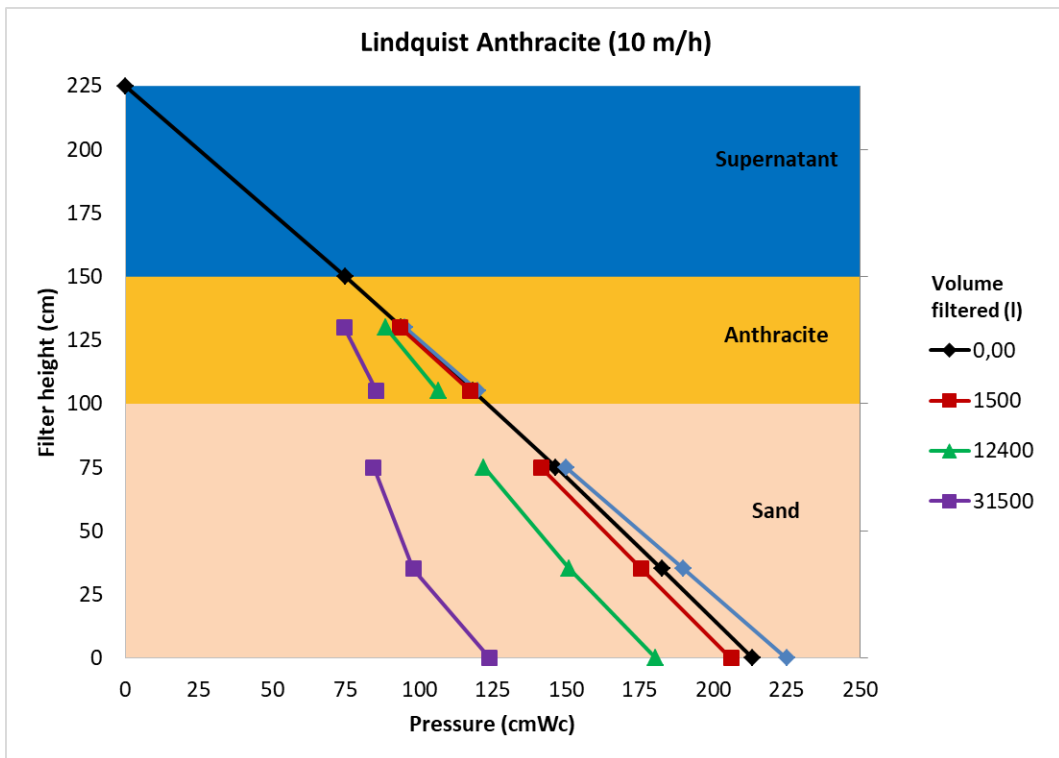


Figure 32: Lindquist diagram of the anthracite filter at a filtration velocity of 10 m/h

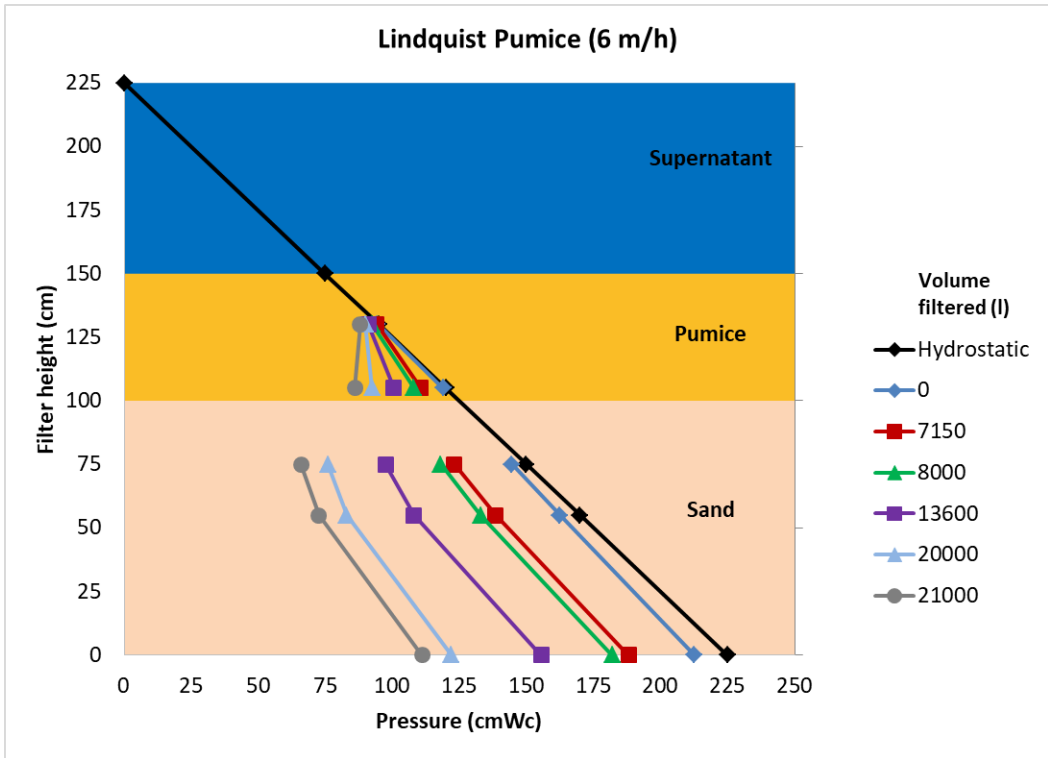


Figure 33: Normalized lindquist diagram of the pumice filter at a filtration velocity of 6 m/h

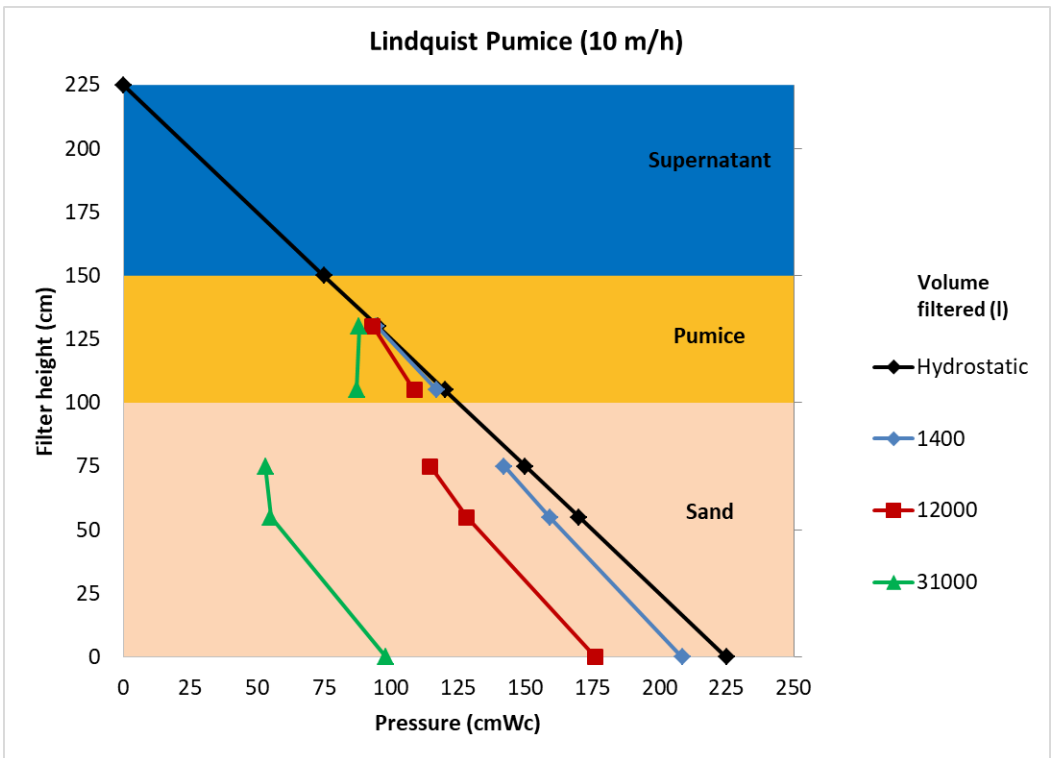


Figure 34: Normalized Lindquist diagram of the pumice filter at a filtration velocity of 10 m/h

### Appendix C: Backwash experiment, samples after 2 minutes of backwashing

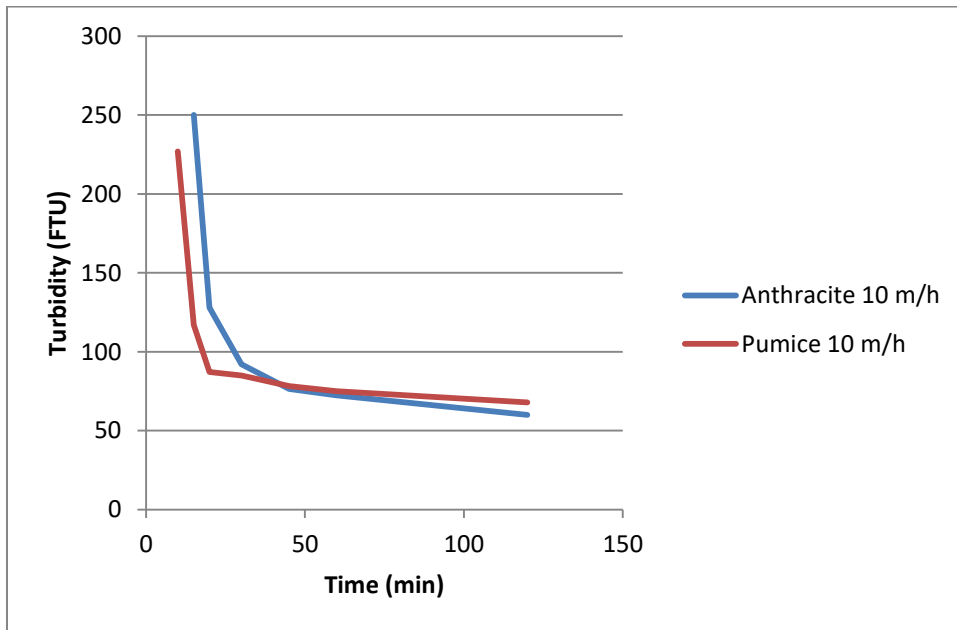


Figure 35: Turbidity at 750 ml (2 minute sample) without the application of AOCF

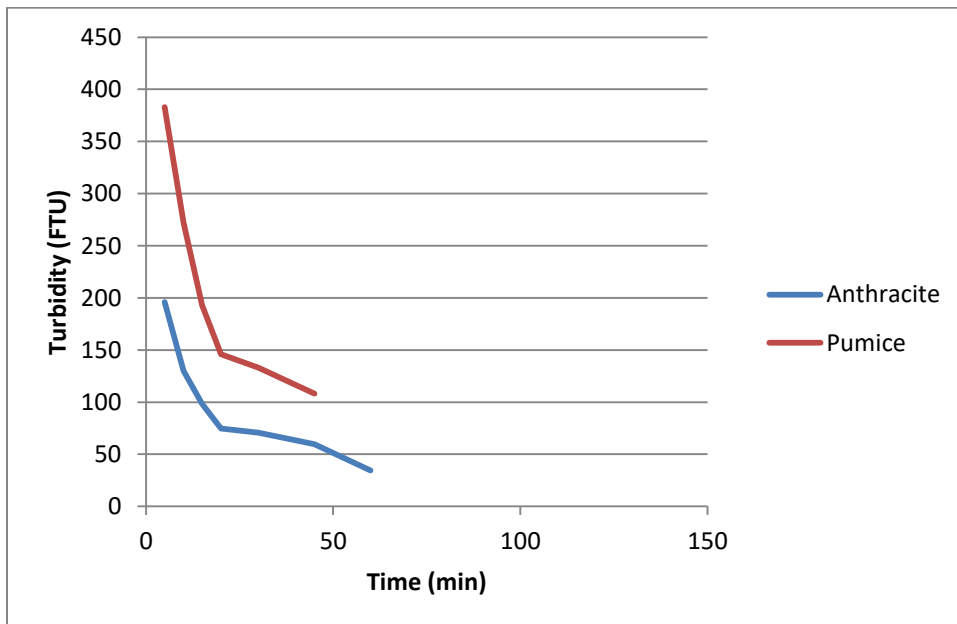


Figure 36: Turbidity at 750 ml (2 minute sample) with the application of AOCF

**Appendice D: Proposal Jar tests for the influence of PAC on effectiveness of  $\text{MnO}_4$  and Fe(III)**

Test 1 Dosing just FeCl<sub>3</sub> (2x without PAC and 2x with PAC (2 mg/L) 4 tests total, 48 samples) (336 WAP)

Dosage	Jar 1	Jar 2	Jar 3	Jar 4	Jar 5
KMnO <sub>4</sub> mg/L (as NaMnO <sub>4</sub> )	0	0.2	0.2	0.2	0.2
FeCl <sub>3</sub> mg/l	0	0.5	1.0	1.5	2.0

Time (t), min	Action	Jar 1	Jar 2	Jar 3	Jar 4	Jar 5	Analysis
t=0	Sample (Unf/Fil/speciation) start solution from the Influent						Analysis for As, Fe
t=0	Start solution in	INF RSF					
t=0	PAC dose	0 mg/l					
t=0	In-situ measurements in start solution	pH, temp, DO					
t=0	Rapid mix start	150 RPM					
t=2	Fe(III) dose	0 mg/L	0.5 mg/L	1 mg/L	1.5 mg/L	2 mg/L	
t=22	Sampling	Unf/Fil	Unf/Fil	Unf/Fil	Unf/Fil	Unf/Fil	Analysis for As, Fe
t=25 - 30 min	In-situ measurements in residual solution	pH, temp, DO					

Test 2 AOCF process (Both settings 2x without PAC and 2x with PAC (2 mg/L) thus 8 tests total, 96 samples) (672 WAP)

Setting 1:

Dosage	Jar 1	Jar 2	Jar 3	Jar 4	Jar 5
KMnO <sub>4</sub> mg/L (as NaMnO <sub>4</sub> )	0	0.2	0.2	0.2	0.2
FeCl <sub>3</sub> mg/l	0	0.5	1.0	1.5	2.0

Setting 2:

Dosage	Jar 1	Jar 2	Jar 3	Jar 4	Jar 5
KMnO <sub>4</sub> mg/L (as NaMnO <sub>4</sub> )	0	0.4	0.4	0.4	0.4
FeCl <sub>3</sub> mg/l	0	0.5	1.0	1.5	2.0

Time (t), min	Action	Jar 1	Jar 2	Jar 3	Jar 4	Jar 5	Analysis
t=0	Sample (Unf/Fil/speciation) start solution from the Influent						Analysis for As, Fe
t=0	Start solution in	INF RSF					
t=0	PAC dose	0 mg/l					
t=0	In-situ measurements in start solution	pH, temp, DO					
t=0	Rapid mix start	150 RPM					
t=2	NaMnO <sub>4</sub> dose	0 mg/l	0.18 mg/l	0.18 mg/l	0.18 mg/l	0.18 mg/l	Equal to 0.2 mg KMnO <sub>4</sub> / L
t=4	Fe(III) dose	0 mg/L	0.5 mg/L	1 mg/L	1.5 mg/L	2 mg/L	
t=22	Sampling	Unf/Fil	Unf/Fil	Unf/Fil	Unf/Fil	Unf/Fil	Analysis for As, Fe
t=25 - 30 min	In-situ measurements in residual solution	pH, temp, DO					

Jar test procedure (Example for setting 1)

Test 3 (executed 2 times, 36 samples) (420 WAP)

Influence of PAC on the oxidation of As(III) by NaMnO<sub>4</sub>

0.5 mg/l NaMnO<sub>4</sub>

Vary the PAC dosage to see the influence of the PAC concentration (0, 1, 2, 3, 4 mg/l) on the oxidation of arsenic by MnO<sub>4</sub>.

Time (t), min	Action	Jar 1	Jar 2	Jar 3	Jar 4	Jar 5	Analysis
t=0	Sample (Unf/Fil/speciation) start solution from the Influent						Analysis for As, Fe and As speciation
t=0	Start solution in	INF RSF					
t=0	PAC dose	0 mg/l	1 mg/l	2 mg/l	3 mg/l	4 mg/l	
t=0	In-situ measurements in start solution	pH, temp, DO					
t=0	Rapid mix start	150 RPM					
t=2	NaMnO <sub>4</sub> dose	0.5 mg/L					
t=22	Sampling	Unf/Fil	Unf/Fil	Unf/Fil	Unf/Fil	Unf/Fil	Analysis for As, Fe and As Speciation
t=25 - 30 min	In-situ measurements in residual solution	pH, temp, DO					

Test 4 (executed 2 times, 24 samples) (336 WAP)

Influence of PAC on the removal capacity of arsenic by Fe(III)

1.0 mg/l Fe(III)

Vary the PAC dosage to see the influence of the PAC concentration (0.5, 1, 2, 3, 4 mg/l) on the arsenic removal capacity of Fe(III)

Time (t), min	Action	Jar 1	Jar 2	Jar 3	Jar 4	Jar 5	Analysis
t=0	Sample (Unf/Fil/speciation) start solution from the Influent						Analysis for As, Fe
t=0	Start solution in	INF RSF					
t=0	PAC dose	0 mg/l	1 mg/l	2 mg/l	3 mg/l	4 mg/l	
t=0	In-situ measurements in start solution	pH, temp, DO					
t=0	Rapid mix start	150 RPM					
t=2	Fe(III) dose	1 mg/L					
t=22	Sampling	Unf/Fil	Unf/Fil	Unf/Fil	Unf/Fil	Unf/Fil	Analysis for As, Fe
t=25 - 30 min	In-situ measurements in residual solution	pH, temp, DO					